

## Review

# Advances in GLP-1 receptor targeting radiolabeled agent development and prospective of theranostics

Irina Velikyan<sup>1</sup>✉ and Olof Eriksson<sup>2</sup>

1. Department of Medicinal Chemistry, Uppsala University, Uppsala, Sweden
2. Science for Life Laboratory, Department of Medicinal Chemistry, Uppsala University, Uppsala, Sweden

✉ Corresponding author: Irina Velikyan, Ph.D., Assoc. prof. PET Center, Center for Medical Imaging, Uppsala University Hospital, SE-751 85 Uppsala, Sweden. Tel. +46 (0)70 4834137; Fax. +46 (0)18 6110619; E-mail: irina.velikyan@akademiska.se

© The author(s). This is an open access article distributed under the terms of the Creative Commons Attribution License (<https://creativecommons.org/licenses/by/4.0/>). See <http://ivyspring.com/terms> for full terms and conditions.

Received: 2019.07.12; Accepted: 2019.09.10; Published: 2020.01.01

## Abstract

In the light of theranostics/radiotheranostics and prospective of personalized medicine in diabetes and oncology, this review presents prior and current advances in the development of radiolabeled imaging and radiotherapeutic exendin-based agents targeting glucagon-like peptide-1 receptor. The review covers chemistry, preclinical, and clinical evaluation. Such critical aspects as structure-activity-relationship, stability, physiological potency, kidney uptake, and dosimetry are discussed.

Key words: Exendin-4, insulinoma, GLP-1, diabetes, PET, SPECT

## Introduction

The pancreatic beta cells are crucial for the body's glucose metabolism. Change in beta cell mass (BCM) is implicated in several disorders, for example decrease in BCM is a hallmark of diabetes, while uncontrolled growth of BCM leads to neuroendocrine cancer [1, 2]. The clinical value of targeting GLP-1R has been demonstrated in diabetes with medicinal products used to stimulate insulin release, and in cancer for diagnostic imaging of e.g. insulinoma tumors. This review presents evolution of agents for Positron Emission Tomography (PET) and Single Photon Emission Computed Tomography (SPECT) imaging of GLP-1R. It addresses the key aspects of the agent chemistry and biological function, biodistribution, dosimetry, and feasibility of theranostics and radiotheranostics. The potential of targeting GLP-1R in the context of personalized medicine wherein GLP-1R targeted imaging provides basis for individualized treatment is discussed. GLP-1 analogues meet the prior prerequisite of high receptor binding specificity, but the major challenging aspects such as high sensitivity and resolution required because of the small size of the cells and consequently

low amount of GLP-1R, and subtle changes that must be quantified demand more attention.

### Unmet medical needs in diabetes

Diabetes affects hundreds of millions of individuals worldwide and the number is expected to double by year 2035 [3-5]. Conventional diagnostic plasma markers such as fasting B-glucose, glycated hemoglobin A1c, insulin, C-peptide levels and oral glucose tolerance tests provide important information on beta cell function, but changes in these parameters are not tightly coupled to changes in BCM. In fact, a significant fraction of BCM may be lost already by the time of diagnosis of diabetes using plasma markers [6, 7]. These methods do not provide direct and quantitative information of the BCM. Moreover, they are an amalgam of the beta cell response to blood-glucose and downstream metabolic processes and may not always provide a sensitive and reproducible assessment of beta cell function either. Thus, there is an unmet need for early and non-invasive diagnostic tool that would support prevention and treatment of the disease. Moreover,

some antidiabetic drugs become ineffective over time and monitoring of the disease status is crucial for the adjustment of the treatment in time. Prediction of the drug efficacy on the individual basis is another value that such method would offer. Islet transplantation is an emerging treatment of type 1 diabetes (T1D) [8], however longitudinal studies are required for the investigation of the islet survival and function during various transplant procedures. Thus, *in vivo* non-invasive imaging technology such as PET would be of utmost importance for monitoring transplanted beta cells [9, 10].

With a continuously increasing population affected by T1D and type 2 diabetes (T2D) worldwide, there is an unmet clinical need for the treatment and prevention of the disease [11]. GLP-1R has been considered a potential target for T2D management since the 1990s. Therapeutic drugs targeting GLP-1R provide glucose control by the incretin effect, i.e. they help the beta cells release increasing amounts of insulin in response to hyperglycemia. Development of novel GLP1R targeting drugs has the potential for improving therapeutic efficacy while reducing side effects (e.g. nausea). However, the drug development process imposes scientific, clinical, and financial challenges. Unfortunately, the failure rate of new drugs, in general, is rather high and it is a costly process. PET offers advantages such as possibility to quantify the target engagement and occupancy very early in the development *in vivo* in humans due to the microdosing concept [12-14] thus facilitating stratification of candidate drugs. The microdosing concept implies that the drug is administered at sub-therapeutic doses often defined as 1% of the expected therapeutic dose or maximally 100 µg (or 30 nanomoles for macromolecules). Microdosing lessens safety requirements and allows Phase 0 trials, potentially reducing the associated cost substantially. Many GLP-1R agonists are highly potent and may exert pharmacological effects already at dose of 10 µg. In this context, very small doses of radiolabeled compound must be administered to follow the microdosing principles.

The development of novel anti-diabetic therapies targeting GLP-1R would benefit from the employment of PET that would enable *in vivo* investigation of GLP-1R engagement by the therapeutic agent. Based on such early and safe *in vivo* drug evaluation in man, it is possible to select or reject the candidate drug optimizing development expenses. Considerable effort is currently directed to the development of dual agonist drugs, e.g. combining activity for both GLP-1 and the glucagon receptor or the gastric inhibitory polypeptide (GIP) receptor [15-18]. Such unimolecular drugs with

several targets would potentially provide improved glucose control combined with clinically meaningful weight reduction. An early target occupancy investigation using PET in combination with radiolabeled ligands for each of the intended target receptors would play an important role in the acceleration of the development process [19]. The level of occupancy of the GLP-1R required for full agonistic effect is not known, but can potentially be studied by PET.

### Unmet medical needs in cancer

Both benign and malignant insulinomas are forms of pancreatic neuroendocrine tumors (PNETs) of beta-cell origin [20-22]. In most of the cases (over 90%) they are benign and single, however very difficult to accurately localize using radiological methods such as endosonography, MR and CT prior to surgical excision due to the small size (1-2 cm) [23-28]. Moreover, the incomplete resection may cause symptom persistence. They cause hyperinsulinemic hypoglycemia, and although they are rare it is a potentially fatal disease. The density of the somatostatin receptors in benign insulinomas is commonly insufficient for diagnostic imaging, e.g. [<sup>111</sup>In]-pentetreotide (Octreoscan®) failed to detect the small multiple lesions in human examinations. Whereas GLP-1R is expressed with high incidence and density opening the possibility for utilizing exendin-based imaging agents for accurate localization and intraoperative guidance [29-33].

The accuracy of staging is crucial in case of malignant insulinomas, and unfortunately conventional radiological procedures such as magnetic resonance (MR) imaging, endosonography, and Computed Tomography (CT)) are conclusive in <50% [27, 34-36]. Selective angiography together with venous sampling for insulin after intra-arterial calcium stimulation administration provides the accuracy of 60-80%, however, it is an invasive procedure with high risk for side effects. Radionuclide-based imaging with metabolic agents such as [<sup>18</sup>F]Fluorodeoxyglucose ([<sup>18</sup>F]FDG)/PET-CT, [<sup>11</sup>C]5-Hydroxytryptophan (5-[<sup>11</sup>C]HTP/PET-CT or [<sup>18</sup>F]DOPA/PET-CT was found insufficiently sensitive [26]. In contrast to benign insulinomas, malignant insulinomas express SSTR in density adequate for the imaging, while GLP-1Rs are expressed to much lesser extent or absent [37]. Nevertheless, both SPECT and PET clinical studies demonstrated imaging of malignant insulinoma using exendin-4 analogues [26, 38, 39]. Targeting both SSTRs and GLP-1Rs could provide complementary diagnostic value wherein negative scan using imaging agents comprising GLP analogues may potentially

indicate malignancy [40].

### Targeting glucagon-like peptide 1 receptor (GLP-1R)

Endogenous GLP-1 exists in two forms, GLP-1(7-36)-NH<sub>2</sub> and GLP-1(7-37)-NH<sub>2</sub> and belongs to the incretin hormone group responsible for the regulation of blood glucose level. The respective receptor, GLP-1R, is a G-protein coupled receptor of seven-transmembrane topology [23, 32, 33, 41]. It is expressed physiologically in pancreas, intestine, lung, kidney, breast and brain, and overexpressed in such pathologies as insulinomas, gastrinomas, and pheochromocytomas with the highest GLP-1R incidence and density in insulinomas [32, 33, 42]. GLP-1R is considerably expressed on the beta cells which constitute approximately 65-80% of the cells in islets of Langerhans, while expression in exocrine pancreas, and other pancreatic endocrine cells (for example, alpha- and delta-cells) has been reported as either absent, low or intermediate in human, depending on study [43-45]. GLP1R mRNA transcription in human exocrine pancreas is low. However, some animal models such as pigs seem to exhibit high GLP1R densities in the exocrine pancreas [46]. The anti-diabetic function of GLP-1 presents therapeutic interest especially in T2D. Additionally, agonism of the GLP1R has been implicated in promoting beta cell proliferation and regeneration in animal models [47]. The major hinder of using endogenous GLP-1 as a drug was its short plasma half-life (< 2 min) [48] and research efforts were directed at the improvement of in vivo stability against dipeptidyl peptidase IV (DPP-IV) and neutral endopeptidase (NEP). It resulted in several anti-diabetic drugs (exenatide/AstraZeneca, liraglutide/Novo Nordisk, taspoglutide/Ipsen-Roche, lixisenatide/Sanofi-Aventis, semaglutide/Novo Nordisk, albiglutide/GalxoSmithKline) based on GLP-1 analogs that stimulate insulin biosynthesis and secretion dependent on the blood glucose level and restoration of beta cell mass and function [18, 49]. Research in molecular targeting of GLP-1R expressed on beta cells [43] and involved in various pathological processes, e.g. in insulinomas, gastrinomas, and pheochromocytomas [23, 32, 33, 41] has been expanding very fast since the development of metabolically stable ligands, e.g. exendin-4. A 39 amino acid residue peptide, exendin-4, isolated from the saliva of Gila monster lizard has plasma half-life of 2.4 h [49, 50]. It binds to the same GLP-1R site as GLP-1 does with picomolar activity [51, 52]. Exendin-4 has 50% homology with GLP1. Crystal structure studies indicated that exendin-4 forms both hydrophobic and hydrophilic interactions with

GLP-1R [52]. The pioneer study of biodistribution of radioiodinated exendin-3 (also a GLP-1R agonist, identical to exendin-4 except for two amino acid substitutions) in rat insulinoma model demonstrated the potential of GLP-1R targeted scintigraphy for the insulinoma detection in vivo [53]. However, exendin-3 and the radiolabel were not sufficiently stable, and the author warranted further research for the improvement, in particular labeling with radiometals.

### Challenges of in vivo beta cell quantification

It is assumed that the investigation of T1D and T2D pathophysiology mechanism requires distinguishing between BCM and beta cell function [7, 54]. Longitudinal invasive tissue sampling of the pancreas to measure BCM by histology is in most circumstances unacceptable due to the complications associated with pancreatic biopsies. Thus, the accurate histochemical determination of the BCM is not normally feasible except in cross-sectional studies using tissue samples from post mortem organ donors. PET and SPECT imaging of beta cells in vivo in humans is challenging since the spatial resolution of the scanners (>4 mm) exceeds at least 10-fold the size of the islets of Langerhans (50-300 μm) comprising beta cells. While this means that it is highly challenging to image individual islets, it is still theoretically and practically feasible to image the beta cell concentration in a given pancreatic volume. Therefore, it is also possible with medical scanners to longitudinally assess the total pancreatic BCM by multiplying the beta cell concentration with the total pancreatic volume. The total mass of beta cells constitutes approximately 2% of the total pancreatic mass and the cells are scattered heterogeneously throughout the pancreatic volume [7, 55]. As in similar applications where the target density in tissue is low (e.g. astrocyte imaging in neuroinflammation), high sensitivity of the imaging technology in combination with high specificity of the labeled ligand compensate for the resolution shortcomings. It is suggested to measure the total pancreatic uptake with prerequisite of specific accumulation solely in the beta cells [54, 56]. Thus, the prospective of the quantification of the BCM is reduced mainly to the availability of high specificity imaging agents. The extensive investigational work has been conducted preclinically using human tissue bank material, various animal species, and <sup>68</sup>Ga-, <sup>111</sup>In- and <sup>177</sup>Lu-labeled exendin analogues, and the uptake of pancreas was shown to correlated with BCM in murine models [57-59]. It is important to stress that as long as GLP-1R is absent on pancreatic acini [57] and islet alpha cells [60] it is feasible to quantify the beta

cell uptake of exendin-4 based analogues with high accuracy, despite the limited resolution of PET and SPECT scanners. It is worth mentioning that no correlation of  $^{177}\text{Lu}$ -labeled exendin-4 uptake and estimated alpha cell mass could be found in a study of transplanted islets in non-diabetic mice [9]. The analogues labeled with positron emitting radionuclides potentially provide advantages in terms of higher sensitivity, resolution, accurate quantification, and determination of kinetic parameters describing the uptake mechanism and thus underlying biological processes.

### Imaging agents: chemistry and pre-clinical evaluation

PET and SPECT present strong potential for the in vivo imaging of subnanomolar imaging agent concentration. It has been of strong interest to develop an imaging agent specifically targeted at GLP-1 receptor for non-invasive and quantitative diagnosis. Since the natural agonist, a 30 amino acid residue hormone, is metabolically unstable [61], analogues with prolonged in vivo half-life have been developed [53, 62, 63]. A more stable GLP-1R agonist, synthetic exendin-4 (Exenatide) is currently used in diabetic treatment. Molecular imaging agents based on

exendin-3 and exendin-4 targeting GLP-1R for SPECT [53, 62-69] and PET [9, 26, 58, 68-87] were developed and demonstrated clinical value of both SPECT [64-66] and PET [26, 59, 75, 87]. Various studies have been conducted with the common aim to develop a targeting agent for specific binding to GLP-1R with high affinity. The most challenging aspects that have been addressed are specific radioactivity, structure-activity relationship, in vitro and in vivo stability, high kidney uptake, and high physiological potency of the ligands. A number of imaging agents varying in the peptide sequence, chelator and prosthetic group moiety, and radionuclide ( $^{18}\text{F}$ ,  $^{64}\text{Cu}$ ,  $^{68}\text{Ga}$ ,  $^{111}\text{In}$ ,  $^{99\text{m}}\text{Tc}$ ,  $^{177}\text{Lu}$ ,  $^{124/125/131}\text{I}$ ,  $^{89}\text{Zr}$ ) has been developed and investigated preclinically and clinically. They demonstrated variability in affinity, pharmacokinetics, and biodistribution. The modulation of kidney uptake was investigated particularly. The respective ligands were labeled with  $^{111}\text{In}$  [63, 68, 69],  $^{99\text{m}}\text{Tc}$  [65, 69],  $^{68}\text{Ga}$  [58, 68, 69, 77, 78], and  $^{64}\text{Cu}$  [71, 77-79],  $^{18}\text{F}$  [72-74, 80-84], and  $^{89}\text{Zr}$  [85]. The choice of a radionuclide is commonly determined by the purpose of a study and critical characteristics such as availability, decay mode, and labeling chemistry (Table 1).

**Table 1.** Radionuclides used for the labeling of exendin analogues in respective fields of PET, SPECT and radiotherapy, their production mode and decay properties.

Radionuclide	Half-life	$E_{\text{max}}$ (keV)	Radiation	Production
<b>Positron emitters</b>				
$^{18}\text{F}$	110 min	634	$\beta^+$ (97%)	Cyclotron
$^{64}\text{Cu}$	12.8 h	656	$\beta^+$ (19%)	Cyclotron
$^{68}\text{Ga}$	67.6 min	1899, 770	$\beta^+$ (89%)	Generator
$^{89}\text{Zr}$	78.4 h	900	$\beta^+$ (23%)	Cyclotron
$^{124}\text{I}$	4.17 d	2100	$\beta^+$ (23%)	Cyclotron
<b>Gamma emitters</b>				
$^{99\text{m}}\text{Tc}$	6.0 h	141	$\gamma$	Generator
$^{111}\text{In}$	67.9 h	245, 172	$\gamma$	Cyclotron
$^{123}\text{I}$	13.3 d	159	$\gamma$	Cyclotron
<b>Therapeutic radionuclides</b>				
$^{131}\text{I}$	8.0 d	1810	$\beta^-$	Fission
$^{177}\text{Lu}$	6.71 d	500	$\beta^-$	Reactor

Radiometals are marked in grey.

## Metal radionuclide-based analogues

Exendin-4 was conjugated to either tetraazacyclododecaneacetic acid (DOTA) or diethylenetriaminepentaacetic acid (DTPA) via amino hexanoic acid linker (Ahx) [62, 63, 69, 88]. [Lys<sup>40</sup>(Ahx-DTPA-<sup>111</sup>In)NH<sub>2</sub>]-exendin-4 demonstrated nanomolar affinity and rapid binding and internalization kinetics in INS-1 cells *in vitro* and high uptake in subcutaneous INS-1 tumors of BALB/c nude mice [67]. The uptake of [Lys<sup>40</sup>(Ahx-DTPA-<sup>111</sup>In)NH<sub>2</sub>]-exendin-4 was also detected in GLP-1R positive organs such as stomach, pancreas, lung, adrenals, and pituitary in healthy rats and mice, while no brain accumulation was detected *in vivo* in mice [62]. The agent not only localized tumors in Rip1Tag2 mouse model of pancreatic beta-cell carcinogenesis [63] but also demonstrated radiotherapeutic effect with up to 94% reduction of the tumor volume in a dose dependent fashion and without significant acute organ toxicity [88]. The strong potential of [Lys<sup>40</sup>(<sup>68</sup>Ga-DOTA)]-exendin-3 and [Lys<sup>40</sup>(<sup>111</sup>In-DTPA)]-exendin-3 for diagnostic imaging of insulinomas was demonstrated in mice bearing INS-1 xenografts and also for the determination of beta cell mass shown in rat model of alloxan-induced beta cell loss [57, 67, 68]. The affinity of [Lys<sup>40</sup>(<sup>111</sup>In-DTPA)]-exendin-3 determined as IC<sub>50</sub> in INS cells was in low nanomolar range [67]. [Lys<sup>12</sup>(<sup>111</sup>In-BnDTPA-Ahx)]-exendin-4 demonstrated specific uptake in mouse pancreatic beta cells and insulinoma xenografts [89, 90].

<sup>99m</sup>Tc presents advantage over <sup>111</sup>In in lower radiation burden and higher resolution. Exendin-4 labeled with <sup>99m</sup>Tc ([Lys<sup>40</sup>(Ahx-HYNIC-<sup>99m</sup>Tc/ethylenediaminediacetic acid [EDDA])NH<sub>2</sub>]-exendin-4) demonstrated significantly lower tumor and organ uptake in Rip1Tag2 mouse model of pancreatic beta cell carcinogenesis compared to <sup>68</sup>Ga and <sup>111</sup>In labeled counterparts, however the quality and contrast of the image was still sufficiently high [69]. The effective dose of [Lys<sup>40</sup>(Ahx-HYNIC-<sup>99m</sup>Tc/EDDA)]-exendin-4 was 43 times less than that for [Lys<sup>40</sup>(Ahx-DOTA-<sup>111</sup>In-NH<sub>2</sub>)]-exendin-4. Two analogues of [Lys<sup>40</sup>(Ahx-HYNIC-<sup>99m</sup>Tc/EDDA)]-exendin-4 containing either methionine or norleucine at position 14 demonstrated similar biodistribution with blockable uptake in GLP-1R positive organs such as lung, pancreas and stomach in normal rats [86]. <sup>99m</sup>Tc-HYNIC-β-Ala-Exedin4 was successfully used to monitor the BCM in mouse model of diet-induced obesity (DIO) and diet-restricted obesity (DRO) wherein DIO considerably reduced the beta cell uptake and DRO failed to normalize the uptake [91]. A GMP compliant freeze-dried kit for the preparation

of <sup>99m</sup>Tc-EDDA/HYNIC)-exendin(9-39) was developed and validated for the clinical use in diagnosis of insulinomas [92].

<sup>111</sup>In and <sup>99m</sup>Tc present such disadvantages as relatively high radiation burden, low spatial resolution and sensitivity as well as poor quantification, that can be overcome by using <sup>68</sup>Ga. Several analogues based on metabolically stable exendin-3 and exendin-4 have been labeled with <sup>68</sup>Ga via such chelator moieties as NOTA, NODAGA, DOTA, and DFO conjugated to the peptides at various positions. They were evaluated preclinically *in vitro*, *ex vivo* and *in vivo* for the feasibility of the visualization and quantification of GLP-1R in tumors and pancreatic beta cells, and some of them were compared to their <sup>111</sup>In-<sup>99m</sup>Tc, <sup>64</sup>Cu- and <sup>86</sup>Zr-labeled counterparts.

[Lys<sup>40</sup>(Ahx-DOTA)NH<sub>2</sub>]-exendin-4 labeled with <sup>68</sup>Ga under microwave heating was biologically evaluated in Rip1Tag2 mouse model of pancreatic beta cell carcinogenesis investigating biodistribution and dosimetry [69]. The target localization and blood clearance were fast visualizing as small as 1.5 and 2.3 mm tumors in the mouse pancreas by a human PET/CT scanner. The uptake of 205±59 %ID/g was significantly higher than that of the <sup>99m</sup>Tc- and <sup>111</sup>In-counterparts. The effective radiation dose for [Lys<sup>40</sup>(Ahx-DOTA-<sup>68</sup>Ga)NH<sub>2</sub>]-exendin-4 was 31.7 μSv/MBq which was 5 times lower and 8 times higher than that for <sup>111</sup>In- and <sup>99m</sup>Tc-counterparts respectively. Exendin-3 labeled with <sup>68</sup>Ga via DOTA conjugated at Lys<sup>40</sup> position, [Lys<sup>40</sup>(<sup>68</sup>Ga-DOTA)]-exendin-3, demonstrated somewhat lower uptake in INS-1 xenografts in mice as compared to [Lys<sup>40</sup>(<sup>111</sup>In-DTPA)]-exendin-3 [68]. However, given the advantages of PET over SPECT, [Lys<sup>40</sup>(<sup>68</sup>Ga-DOTA)]-exendin-3 was considered as a promising PET imaging agent.

Another analogue comprising DOTA chelator moiety conjugated to exendin-4 at Cys<sup>40</sup> position was labeled with <sup>68</sup>Ga by both manual and automated procedure [46, 58, 70, 93-95]. Exendin-4 containing methionine was susceptible to radiolytic oxidation that was suppressed while maintaining relatively high radiochemical yield by fine optimization of the combination of radical scavengers and heating temperature [93]. During labeling with <sup>177</sup>Lu, where the radiolysis is stronger, the stability of [<sup>177</sup>Lu]Lu-DO3A-VS-Cys<sup>40</sup>-exendin-4 was achieved by using smaller amount of <sup>177</sup>Lu and adding ascorbic acid also to the final product that was stable for at least a week at -20 °C. GLP-1R-mediated uptake of [<sup>68</sup>Ga]Ga-DO3A-VS-Cys<sup>40</sup>-exendin-4 in rat pancreas *in vivo* was demonstrated by co-administration of cold peptide in excess [58]. Moreover, the pancreatic

uptake decreased in streptozotocin (STZ) diabetic animals with selectively ablated beta cells. It was possible to clearly distinguish between pancreatic endocrine tumor (INS-1) and pancreatic exocrine tumor (PANC1) xenografts [70]. The proximity to the kidneys and diffused shape of the pancreas and difficulty of its anatomical identification precluded *in vivo* quantification of the uptake reduction in rats. Instead, streptozotocin-induced diabetic pigs were considered for the *in vivo* studies of GLP-1R as an imaging biomarker of beta cell mass [94]. However, no meaningful difference could be detected in the uptake between non-diabetic animals and pigs with STZ induced diabetes with verified complete loss of beta cells [26, 94]. Thus, the pancreatic distribution of GLP-1R seems to differ radically in pigs compared to rats, with more expression in the exocrine pancreas. Interestingly, the pigs experienced dose dependently increased heart rate after administration of [<sup>68</sup>Ga]Ga-DO3A-VS-Cys<sup>40</sup>-exendin-4 [96, 97] to a degree which usually not seen in other species. Strong pancreatic binding of [<sup>68</sup>Ga]Ga-DO3A-VS-Cys<sup>40</sup>-exendin-4 was also observed in cynomolgus monkeys (NHP). The binding in NHP pancreas was GLP1R mediated, as it could be progressively competed away dose dependently by co-injection of unlabeled DO3A-VS-Cys<sup>40</sup>-exendin-4 [58]. Using <sup>177</sup>Lu as a proxy for <sup>68</sup>Ga in *in vitro* studies utilizing its higher spatial resolution, it was shown that DO3A-VS-Cys<sup>40</sup>-exendin-4 binds specifically to intramuscularly transplanted islets in mice [9]. Thus, DO3A-VS-Cys<sup>40</sup>-exendin-4 radiolabeled with a suitable radiometal is potentially a marker for visualization also of transplanted islets at different sites. *Ex vivo* autoradiography of sections of explanted pancreata was performed in mouse, rat, pig and NHP after administration of <sup>68</sup>Ga or <sup>177</sup>Lu labeled DO3A-VS-Cys<sup>40</sup>-exendin-4. The correlation of binding in the islets was demonstrated by insulin staining of consecutive sections (Figure 1). Interestingly, the islet-to-exocrine ratio varied between species, with the

highest contrast – and thus the best promise for pancreatic islet visualization – was seen in rat, followed by mouse and NHP [46]. The islet-to-exocrine contrast in pig pancreas was poor, approaching 1 (i.e. similar GLP1R density in the endocrine and exocrine pancreas).

An exendin-4 analogue, wherein the methionine was substituted with norleucine and NODAGA chelator moiety was introduced instead of DOTA (Nle<sup>14</sup>, Lys<sup>40</sup>(Ahx-NODAGA-<sup>68</sup>Ga)NH<sub>2</sub>)-exendin-4), was investigated with the objective to visualize rat pancreatic islets [78]. The IC<sub>50</sub> value determined in cell was in nanomolar range (2.17 ± 0.42 nM) however the author concluded that *in vivo* imaging of beta cell in rats could not be achieved, due to strong spill-in of signal from kidneys. The same analogue demonstrated relatively high blood and healthy organ uptake with highest values for GLP-1R positive lung and kidney 1 h post injection in rats [86]. Three analogues of exendin-4 comprising NODAGA chelator moiety conjugated to Lys residue at position 12 (<sup>68</sup>Ga-Ex4NOD12), 27 (<sup>68</sup>Ga-Ex4NOD27) or 40 (<sup>68</sup>Ga-Ex4NOD40) where preclinically evaluated with the aim to elucidate the importance of the Lys residues for the biological activity of exendin-4 [77]. All three analogues showed specific nanomolar binding in CHL-GLP-1R positive cells and respective xenografts in mice, however <sup>68</sup>Ga-Ex4NOD12 and <sup>68</sup>Ga-Ex4NOD40 were found preferable.

Exendin-4 analogue, comprising leucine at position 14 and NOTA-conjugated Met-Val-Lys sequence added to Cys<sup>40</sup> (NOTA-MVK-Cys<sup>40</sup>-Leu<sup>14</sup>-exendin-4), was developed with the objective to reduce kidney uptake [98]. It was labeled with <sup>68</sup>Ga yielding an agent of high affinity determined in INS-1 cell culture and high tumor uptake determined in INS-1 mouse xenografts, with the performance comparable to that of a control agent without cleavable Met-Val-Lys sequence. While the kidney uptake was reduced considerably.

An analogue of exendin-4 functionalized with

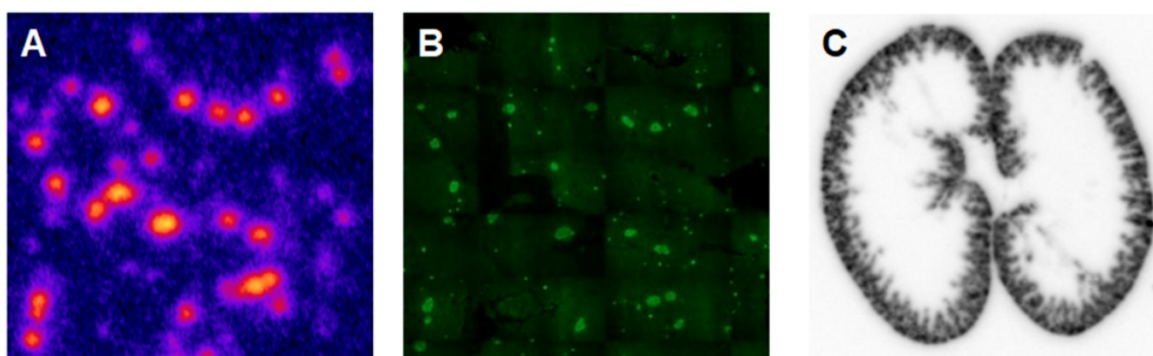


**Figure 1.** *Ex vivo* autoradiography of [<sup>177</sup>Lu]Lu-DO3A-VS-Cys<sup>40</sup>-exendin-4 in rat pancreas and kidney. Autoradiograms of the pancreas revealed a heterogenous focal uptake pattern (A), which corresponded to insulin positive islets of Langerhans (B). The renal uptake and retention were localized primarily to the kidney cortex (C).

DFO instead of DOTA, unexpectedly could not be labeled with  $^{68}\text{Ga}$  at room temperature or at elevated temperature using conventional heating block, but required microwave reactor at  $95\text{ }^\circ\text{C}$  for 1 min [85]. The resulting agent, [Lys $^{40}$ (Ahx-DFO- $^{68}\text{Ga}$ )NH $_2$ ]exendin-4, demonstrated nanomolar receptor affinity, high serum stability and specific in vivo accumulation in nude mice bearing RIN-m5F xenografts. Labeling of [Lys $^{40}$ (Ahx-DFO)NH $_2$ ]exendin-4 with  $^{89}\text{Zr}$ , in contrast to the microwave-assisted labeling with  $^{68}\text{Ga}$ , could be achieved at room temperature within 2 h, however the quantitative complexation required up to 14-16 h [85]. The biological performance of the two analogues was comparable. The longer half-life of  $^{89}\text{Zr}$  allowed for wider time window for monitoring the biodistribution and revealed long kidney retention time with only 30-40% of the administered radioactivity cleared after 48 h.

Exendin-4 labeled with  $^{64}\text{Cu}$  using DOTA chelator derivative,  $^{64}\text{Cu}$ -DO3A-VS-Cys $^{40}$ -exendin-4, showed specific uptake in mouse INS-1 xenografts, as well as high uptake in pancreas and liver [79]. Two analogues with NODAGA chelator moiety wherein in one analogue the chelator was directly coupled to the peptide and in the other one it was coupled via renal enzyme-cleavable N $\epsilon$ -maleoyl-L-lysyl-glycine (MAL) linker with the aim to reduce the kidney uptake were studied in rats [99]. However, the biodistribution in healthy animals were similar in the major organs including kidneys indicating no influence of the MAL linker. Nevertheless, the specific GLP1R-mediated binding to the pancreatic tissue sections was maintained. The DOTA and NOTA based complexes with Cu(II) are not sufficiently stable and more stable cross-bridged chelators have been introduced [100]. Bicyclic cage-like chelator (sarcophagine, Sar) forming in vivo stable complex with Cu(II) was used to design monomeric ( $^{64}\text{Cu}$ -BaMalSar-exendin-4) and dimeric exendin-4 ( $^{64}\text{Cu}$ -Mal2Sar-(exendin-4) $_2$ ) agents [71]. The binding affinity determined in INS-1 cells and subcutaneous INS-1 tumor uptake in mice were higher for the dimeric counterpart. Both agents showed high liver and kidney uptake. Bimodal imaging probe based on exendin-4 and bearing Sar chelator moiety for  $^{64}\text{Cu}$ -labeling and near-infrared fluorescent dye moiety was tested in vivo and ex vivo [101]. Specific binding was demonstrated in mice bearing INS-1 xenografts and the pancreatic beta-cell visualization was achieved by both phosphor autoradiography and fluorescent imaging. [Nle $^{14}$ , Lys $^{40}$ (Ahx-NODAGA- $^{64}\text{Cu}$ )NH $_2$ ]-exendin-4 comprising norleucine instead of methionine and NODAGA chelator moiety demonstrated GLP-1R mediated binding to islets in rat pancreatic tissue in vitro,

however in vivo imaging could not be achieved [78].

### Halogen radionuclide-based analogues

The half-life of 110 min and decay mode with 97% positron emission make  $^{18}\text{F}$  a very attractive radionuclide. However, most of the  $^{18}\text{F}$ -labeled exendin analogues demonstrated relatively high non-specific uptake in liver and intestines in animal studies mostly dependent on the labeling methodologies [72-74, 83, 84]. Another challenge is the requirement for high specific radioactivity of 200 GBq/ $\mu\text{mol}$  [102]. The radiolabeling can be accomplished via: conjugation of the peptide to a  $^{18}\text{F}$ -bearing prosthetic group; click chemistry wherein non-saturated component or tetrazine can comprise  $^{18}\text{F}$  or be conjugated to the peptide; and peptide comprising a chelator moiety for the complexation with  $[\text{Al}^{18}\text{F}]^{+2}$ . In the first two procedures an exendin analogue is conjugation to the radiolabeled group and in the latter case the conjugation to the chelator moiety is conducted prior to the labeling with  $[\text{Al}^{18}\text{F}]^{+2}$ . A potential advantage of using  $^{18}\text{F}$  as a radiolabel is the faster washout from the kidney cortex, thereby decreasing the local radiation dose as well as enabling less spillover of the signal into the pancreas in rodent models.

A novel GLP-1 analog, EM3106B, with two cyclic lactam bridges was developed to enhance the biological half-life of the ligand [73, 74]. The constrained structure resulted in improved receptor activation capability and resistance against enzymatic degradation. It was labeled with  $^{18}\text{F}$  via maleimide-based prosthetic group, N-2-(4- $^{18}\text{F}$ -fluorobenzamido)ethylmaleimide ( $^{18}\text{F}$ FBEM) and was used for PET imaging to visualize insulinoma tumors in an animal model. The tracer was tested in nude mice bearing subcutaneous INS-1 insulinoma tumors with GLP-1R and MDA-MB-435 tumors of melanoma origin with low GLP-1R expression. The uptake was correlated with the receptor expression degree. The tracer was excreted both hepatically and renally. Exendin-4 analogue modified with cysteine for site specific labeling via  $^{18}\text{F}$ FBEM,  $^{18}\text{F}$ FBEM-[Cys $^{40}$ ]-exendin-4, was studied also in INS-1 xenografted mice [74]. The uptake in the tumor was high however abdominal persistent background could complicate the localization of pancreatic uptake. The attachment of  $^{18}\text{F}$ FBEM via Cys $^{39}$  of exendin-4 reduced the abdominal background and provided better contrast in mouse xenografts [103]. Similar constructs ( $^{18}\text{F}$ FPeM-[Cys $^{40}$ ]-exendin-4 [81] and  $^{18}\text{F}$ FNEM-[Cys $^{40}$ ]-exendin-4 [82], wherein instead of  $^{18}\text{F}$ FBEM prosthetic groups N-5- $^{18}\text{F}$ fluoropentylmaleimide ( $^{18}\text{F}$ FPeM) and N-(2-(2,5-dioxo-2,5-dihydro-1H-pyrrol-1-yl)-ethyl)-6-fluoronicotinamide ( $^{18}\text{F}$ FNEM)

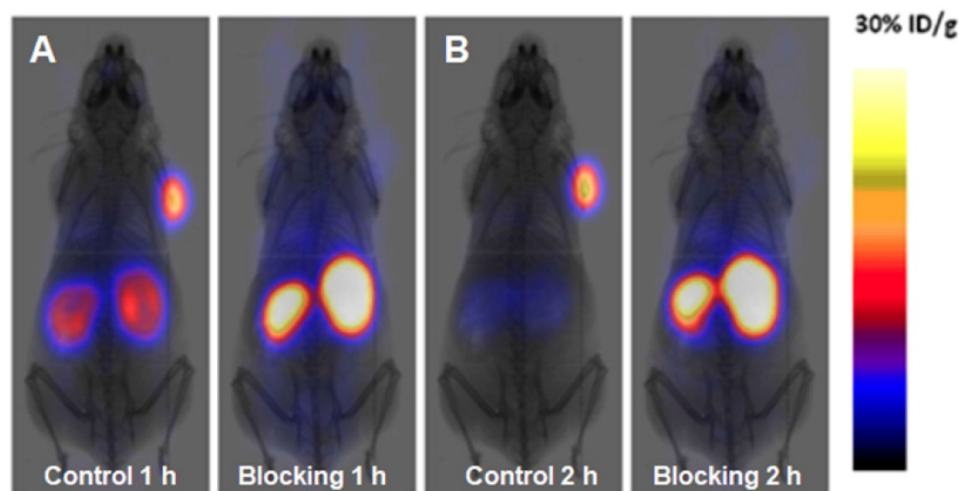


**Figure 2.** PET images of INS-1 tumor mice at 1 (A) and 2 h (B) post injection of [ $^{18}\text{F}$ ]FNEM-[Cys $^{40}$ ]-exendin-4 (30  $\mu\text{Ci}$ ) for the control and blocking groups ( $n = 5/\text{group}$ ). Reproduced from [82].

were used, demonstrated comparable biological properties with high tumor uptake and fast liver and kidney clearance [81, 82]. Amongst the analogues [ $^{18}\text{F}$ ]FNEM-[Cys $^{40}$ ]-exendin-4 presented advantage of more efficient labeling, and fast kidney clearance wherein the uptake decreased to 2.5 %ID/g within 2 h (Figure 2). Silicon containing exendin-4 was labeled with  $^{18}\text{F}$  via one-step nucleophilic substitution [104]. Visualization of mouse pancreas and xenografts was achieved within 2 h post injection. Four exendin (9-39) analogues were labeled with  $^{18}\text{F}$  via amino acid residues at positions 9, 12, 27, and 40 and N-succinimidyl-4-[ $^{18}\text{F}$ ]fluorobenzoate [105]. The analogue labeled at Lys $^{40}$  ([ $^{18}\text{F}$ ]FB40-Ex(9-39)) demonstrated the highest uptake in mouse pancreas.

Chelator-mediated Al $^{18}\text{F}$ -labeling of exendin-4 resulted in an agent, [ $^{18}\text{F}$ ]AlF-NOTA-MAL-Cys $^{40}$ -exendin-4, with high specificity towards GLP-1R demonstrated in mouse INS-1 xenografts [80]. The ex vivo analysis of the plasma and tumor detected intact agent 1 h post injection while content in the kidney and urine was presented by one polar radioactive component. The highest uptake in the tumor was achieved within 5 min while uptake in the kidney continued to increase during 1 h and showed high values that could be reduced by 25% by co-administration of polyglutamic acid solution. However, it was still higher than that of [ $^{18}\text{F}$ ]FBEM-[Cys $^{40}$ ]-exendin-4 and [ $^{18}\text{F}$ ]FPenM-[Cys $^{40}$ ]-exendin-4). [ $^{18}\text{F}$ ]AlF-NOTA-MAL-Cys $^{39}$ -exendin-4 also demonstrated specific binding in vivo in mouse xenografts and kidney uptake [106] higher than that of  $^{18}\text{F}$ -FBEM-Cys $^{39}$ -exendin-4 [103].

The insignificance of lysine residue for the binding of exendin-4 to GLP-1R [52] opened possibility for the functionalization of exendin-4 at Lys $^{12}$  position with cysteine conjugated tetrazine for

the subsequent labeling with  $^{18}\text{F}$ -trans-cyclooctene via click-chemistry [107]. The resulting imaging agent demonstrated uptake in beta cells in vivo, in mouse models of insulinomas as well as in intestine and kidneys. Another exendin-4 analogue comprising norleucine at position 14 and functionalized with azide at Lys $^{40}$  was labeled with  $^{18}\text{F}$  via copper-catalyzed click chemistry [108]. High and specific uptake was observed in rat pancreatic islets. Construct comprising exendin-4 and  $^{18}\text{F}$ -fluorobenzoate demonstrated specific binding in vitro in the insulinoma cell line and in vivo in mice bearing insulinoma xenografts [83]. The tumor was visualized however the background uptake particularly in the abdominal organs was too high. Lower liver background uptake of  $^{18}\text{F}$ -tetrazine trans-cyclooctene (TTCO)-Cys $^{40}$ -exendin-4 allowed visualization of islet grafts in the liver of islet-transplanted mice [84]. The binding specificity was confirmed in INS-1 tumor bearing mice. The kidney uptake was reduced compared to  $^{64}\text{Cu}$ -labeled analogues.

GLP-1R antagonist, exendin(9-39) was labeled with  $^{125}\text{I}$  using Bolton-Hunter reagent ( $^{125}\text{I}$ -BH-exendin(9-39)) conjugated to the peptide via lysine residues [109-111]. Lysine residues were found critical for the binding of  $^{125}\text{I}$ -BH-exendin(9-39) to GLP-1R studied preclinically. BH labeling at Lys $^{19}$  position resulted in similar affinities to both mouse and human GLP-1 receptors, while agent labeled at Lys $^4$  position detected only mouse GLP-1 receptors. Another analogue of exendin(9-39) with norleucine at position 14 was labeled with  $^{125}\text{I}$  via Tyr $^{40}$  residue ([Nle $^{14}$ , $^{125}\text{I}$ -Tyr $^{40}$ -NH $_2$ ]Ex (9-39)) [112]. Despite high affinity, the uptake of [Nle $^{14}$ , $^{125}\text{I}$ -Tyr $^{40}$ -NH $_2$ ]Ex (9-39) in INS-1E xenografts in mice was low and transient. In the contrary, the counterpart analogues based on

exendin-4 demonstrated high specific uptake in the xenografts. Liraglutide comprising tyrosine amino acid residue was labeled with  $^{125}\text{I}$  using iodogen method [113]. The authors hypothesized that the higher homology with GLP-1 (97%) would provide higher sensitivity and specificity to GLP-1R as compared to exendin-4. The specific binding in lung, tumor and pancreas was observed, however the uptake in the background abdominal organs was also high in nude mice with INS-1 xenografts.

### Structure-activity relationship

Multiple GLP-1 analogues were developed for the structure-activity relationship and enzymatic degradation stability studies. The vast data was thoroughly reviewed previously [15]. The importance for specific GLP-1R binding of amino acid residues affected by DPP-IV and NEP was investigated. The sensitive residues were substituted with *D*-amino acids,  $\beta$ -amino acids, and alkylated, glycosylated or halogenated amino acids. Residues with key physicochemical properties were also substituted or functionalized for improved in vivo stability and renal clearance as well as for radioactive labeling. The influence of the chelator position in exendin-4 on the binding and biodistribution of the agents was studied in vitro in GLP-1R transfected cells and ex vivo in mice bearing CHL-GLP-1R positive tumor [77]. The analogues with chelator (NODAGA) conjugated via lysine at position 12, 27 or C-terminus maintained their binding specificity with comparable affinity. The modification at position 27 was considered less preferable. The binding specificity was deteriorated when exendin(9-39) was labeled with  $^{18}\text{F}$  via Lys<sup>27</sup> [72]. The computational investigation of exendin-4 interaction with GLP-1R in the presence of water using MembStruk method demonstrated the importance of both lysine residues for the binding affinity of the ligand [114]. However, the modification at Lys<sup>12</sup> position, [Lys<sup>12</sup>( $^{111}\text{In}$ -BnDTPA-Ahx)] exendin-4, did not deteriorate the binding capability [89].

### Radiolytic stability

Exendin-4 contains methionine and tryptophan amino acid residues that are prone to oxidation especially under labeling conditions using high amount of radioactivity and elevated temperature. This results in formation of oxidized by-product compromising the purity of the radiopharmaceutical. The change in biological activity, in particular receptor binding affinity upon the oxidation can be expected and it is an important task to investigate the issue. Exendin-4 based analogues, comprising methionine or norleucine or oxidized methionine

amino acid residue and labeled with  $^{99\text{m}}\text{Tc}$  were generated and their physicochemical and biological properties were investigated [86]. Oxidized product maintained binding capability though to somewhat lesser extent as compared to the intact counterpart. Although the oxidized form was more hydrophilic, the binding capacity was comparable to that of non-oxidized counterpart.

The radiolytic oxidation can be suppressed by radical scavengers such as ethanol, ascorbic acid, gentisic acid, HEPES, selenomethionine, sodium thiosulfate, L-methionine, etc. [77, 93, 115]. The concentration of the radical scavengers requires optimization, e.g. higher amount of ascorbic acid deteriorates the radiolabeling with  $^{68}\text{Ga}$ , while gentisic acid shows less influence on the reaction efficiency [93]. Another factor that impacts the extent of the radiolysis is the peptide precursor concentration [93]. Increased concentration may decrease the radiolysis. However, complete elimination of the oxidized product is difficult to achieve since the precursor solution might contain the oxidized form, building up during the storage, prior to the labeling. The stability of dry HYNIC-Met<sup>14</sup>-Exendin-4 during the storage was improved in the presence of L-methionine [86]. In the best-case scenario, a single radiochemical entity is preferred. However, the comparable binding capacity would allow the calculation of the radiochemical purity as a sum of the two components. Nevertheless, attempts to decrease the formation of the oxidized product must be conducted until the options are exhausted.

Another solution to improve the radiolytic stability of exendin analogues was the substitution of methionine with its isosteric analogue, norleucine [78, 86, 116]. The replacement of methionine by norleucine improved the binding capability [86]. The biodistribution pattern of the analogues was similar. Exendin-4 contains also Trp however the corresponding by-products have not been investigated yet and given the fact that after the substitution of the Met with Nle the labeling results in a single product it is plausible that the oxidation of Trp under those conditions does not occur.

### Specific radioactivity

Specific radioactivity (SRA) can in general terms be defined as concentration of a radioactive material in a sample (e.g. Bq/mol). The importance of SRA of an imaging agent for enabling high contrast imaging of high affinity/specificity targets and adequate quantification of the target expression as well as to reduce pharmacological and toxic effects is an established knowledge [117]. It is particularly crucial

in the case of in vivo beta cell imaging and quantification wherein the density of GLP-1R is rather low and the agonist ligands are of high potency. Preclinical studies, investigating imaging agent uptake as a function of administered total peptide dose, demonstrated that the total amount of exendin-3/exendin-4 peptide that can be administered to mice and rats in order to provide adequate imaging of pancreatic beta cells should not exceed 20 pmoles [58, 63, 68]. Optimal targeting of subcutaneous INS-1 tumors in BALB/c nude mice corresponded to less than 0.1 µg of [Lys<sup>40</sup>(<sup>111</sup>In-DTPA)]Exendin-3 [68]. The highest pancreatic uptake in rats corresponded to 0.1 µg/kg of <sup>68</sup>Ga-DO3A-exendin-4 [58]. It is possible that even lower mass doses may have yielded higher pancreatic uptake, but the specific radioactivity (SRA) in combination with the small size of the rats limited the minimal doses to 0.1 µg/kg. Finally, dose escalation studies in NHP demonstrated optimal pancreatic binding of <sup>68</sup>Ga-DO3A-exendin-4 for injected peptide mass doses below 0.2 µg/kg. The peptide mass should be associated with radioactivity amount that would provide statistically sufficient counts for detection putting demand on SRA value.

In order to enhance SRA and enable detection and quantification of small changes in beta cell mass responsible for diabetic pathophysiology progression, a number of exendin-3 analogues carrying one, two, or six DTPA moieties were developed [118]. The analogues were labeled with <sup>111</sup>In and the one comprising six chelator moieties demonstrated 7-fold increase in SRA. It maintained its biological activity towards GLP-1R and demonstrated enhanced radioactivity counts in mice and rats with 3-fold improvement of the image contrast and pancreas visualization.

### Animal models

The biological evaluation of various agents was performed using cell cultures (INS-1, islets), tissue section autoradiography (pancreas, INS-1 xenograft sections), ex vivo and in vivo biodistribution in healthy animals (mouse, rat, pig, non-human primate) and animal models of metabolic disease including nonobese diabetic (NOD) mice, ob/ob mice, biobreeding diabetes-prone rats, Zucker diabetic fatty rats, alloxan, diphtheria toxin or STZ induced diabetes in rodents and pigs.

The possibility of in vivo longitudinal imaging of implanted islets is of utmost importance not only for monitoring the survival and function maintenance of engrafted islets but also for the adjustment of immunosuppressive regime and assessment of novel transplantation sites. Revascularization is essential for

the survival of the engrafted islets following transplantation, and for the tissue perfusion and accessibility of the intravenously administered imaging agents and therapeutics. Targeting GLP-1R was demonstrated relevant for the in vivo imaging. The correlation was found between the formation of the microvasculature in transplanted islets and the uptake of [Lys<sup>40</sup>(DTPA-<sup>111</sup>In)]-exendin-3 in mice the islets transplanted into the calf muscle [119]. The intra-islet vasculature was perceptible after 2 weeks and grew further within 6 weeks of the study penetrating from the periphery into the core of the transplant. Preclinical ex vivo study demonstrated feasibility of beta-cell mass quantification in intramuscular islet grafts in mice using [<sup>177</sup>Lu]DO3A-VS-Cys<sup>40</sup>-exendin-4 [9]. Linear correlation between the radioactivity uptake and the number of transplanted islets was found. The islet-to-background signal ratio was high (40) and the binding in individual islets was similar to that of pancreatic islets.

Human islets intraportally transplanted into NOD/SCID mouse livers via portal vein (i.e. currently the clinically relevant site) were visualized by <sup>64</sup>Cu-DO3A-VS-Cys<sup>40</sup>-exendin-4 [79] and <sup>18</sup>F-TTCO-Cys<sup>40</sup>-exendin-4 [84] and the uptake correlated with the number of the transplanted islets. The uptake of <sup>177</sup>Lu-labeled analogue, [<sup>177</sup>Lu]DO3A-VS-Cys<sup>40</sup>-exendin-4, was correlated with gradually increasing number of islets ingrafted into the abdominal muscle of nondiabetic mice thus demonstrating potential for the in vivo quantification of beta cell mass [9]. The high resolution of the ex vivo tissue autoradiography images allowed accurate correlation of the <sup>177</sup>Lu signal with insulin location determined by immunohistochemistry.

<sup>111</sup>In-labeled exendin-3 was used to determine beta cell mass in mouse and rat models for spontaneous T1D, and demonstrated reduced uptake as compared to the healthy animals [120]. Interestingly, the uptake in the exocrine pancreas was relatively higher in mice compared to rats. Exendin-3 analogue labeled with <sup>111</sup>In, [Lys<sup>40</sup>(<sup>111</sup>In-DTPA)]exendin-3, was tested in a rat model of alloxan-induced beta cell loss [57] and diphtheria toxin induced beta loss in RIP-DTR mouse model [121] wherein the in vivo uptake correlated with beta-cell mass. A rat model of alloxan-induced beta cell loss was found to have less exocrine background binding as compared to the mouse model [122]. However, it is not clear which model that best translate to the human situation and the binding of exendin-4 in the human exocrine pancreas. The accumulation of [Lys<sup>40</sup>(<sup>111</sup>In-DTPA)]exendin-3 in the exocrine pancreas in mice was argued to be mediated

by receptors other than GLP-1R, but this was based on mRNA transcription analysis of isolated islet and exocrine pancreatic compartments, rather than GLP1R density assessment. Conversely, in a recent study by Khera and colleagues, it was demonstrated that exendin-4 binding is indeed mediated exclusively by GLP1R expression in the exocrine pancreas in mouse [123].

Brown Norway rat model was found optimal due to the favorable pancreas-to-background uptake ratio. The uptake of [ $^{64}\text{Cu}$ ]-DOTA-NH<sub>2</sub>-exendin-4 in islet cells was considerably reduced in Zucker diabetic fatty rats [124]. On the other hand, the uptake of [ $^{68}\text{Ga}$ ]DO3A-VS-Cys<sup>40</sup>-exendin-4 was increased in pancreatic islets in mice with mutations in the MEN1 tumor suppressor gene [125]. Radiolabeled exendin-4 therefore seems to be able to distinguish between a large continuous spectrum of aberrantly regulated beta cells, from low binding in islets in T1D/ T2D, via normal uptake to unaffected beta cells, to somewhat increased binding in MEN1 deficient islets onto strong binding in insulinoma cells. This is particularly evident in mouse and rat islets, and it is crucial to take into consideration the biological differences in pancreatic distribution of GLP1R amongst various species, when interpreting the aforementioned results (Figure 3). Importantly, it is currently not clear which animal model best capitulates the situation in the human exocrine pancreas. Different GLP-1R directed polyclonal antibodies have produced variable results regarding the existence or extent of GLP1R in exocrine pancreas or pancreatic ductal cells [43, 45]. In most

studies, beta cells exhibit strong antibody staining. Single cell or small cell clusters close to the ductal epithelium were identified as strongly GLP1R positive and these cells were frequently also insulin positive. Kirk et al also found a relevant proportion of exocrine cells to be GLP1R positive, but with an intensity a third of the beta cells [45]. This islet-to-exocrine ratio of 3 is incidentally in line with the ratios seen in mouse (islet-to-exocrine ratio 4.3) and NHP (islet-to-exocrine ratio 5.3) as determined by *ex vivo* autoradiography with [ $^{177}\text{Lu}$ ]Lu-DO3A-VS-Cys<sup>40</sup>-exendin-4 (Figure 3) [46]. These studies taken together indicate that mouse and NHP animal models may constitute suitable approximations of the expression of GLP1R in human exocrine tissue. Additionally, this indicates that the residual pancreatic signal seen for [Lys<sup>40</sup>(Ahx-DTPA-<sup>111</sup>In)NH<sub>2</sub>]-exendin-4 also in human subjects with long-standing T1D is due to the exocrine binding to GLP1R [57]. Assuming that the exocrine signal constitutes an obstacle for accurate visualization of the beta cells, Khera et al suggested to pretreat mice with lipophilic Cy7-exendin4 to preblock especially the exocrine population of GLP1R. After the pretreatment, sufficient amount of GLP1R remained on the beta cells, which then could be imaged with fluorescent or <sup>111</sup>In-exendin-4 [123].

Moreover, GLP-1R was considered as a biomarker to assess its cardioprotective effect of attenuation of myocardial inflammatory response and fibrosis after ischemic injury [126, 127]. Myocardial ischemia and reperfusion (MI/R) rat models were

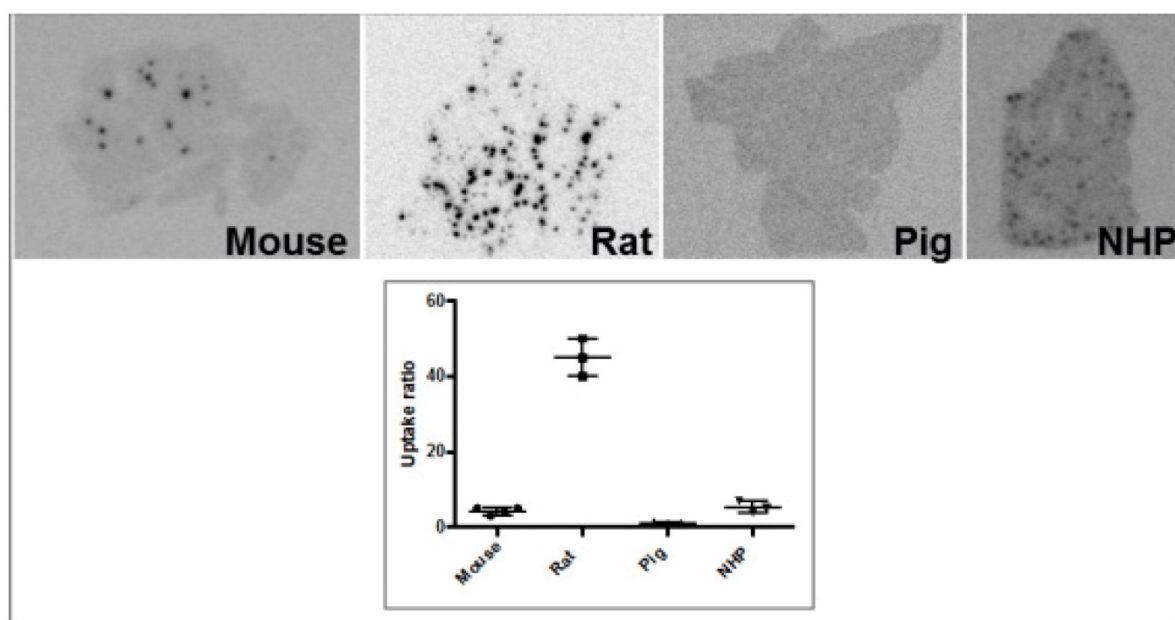


**Figure 3.** Ex vivo autoradiograms of pancreas in vivo distribution of [ $^{177}\text{Lu}$ ]Lu-DO3A-VS-Cys<sup>40</sup>-exendin-4 in mouse, rat, pig, and non-human primate. The islet contrast (graph) defined as the islets-to-exocrine pancreas (IPR, Uptake ratio) ratio was highly dependent on the species (mouse=4.3±1.0, rat=45±5, pig=1.1±0.2, NHP=5.3±1.5), mainly reflecting the difference in background binding. Error bars represent standard deviation (n=3-4).

used. The rapid enhancement of GLP-1R expression upon ischemia-reperfusion was detected using  $^{18}\text{F}$ -FBEM-Cys $^{40}$ -exendin-4 in rats [126]. The results open possibility for the optimization of the therapeutic intervention time schedule. Kinetic modelling of the enhanced uptake of  $^{68}\text{Ga}$ -NODAGA-exendin-4 in the infarcted area in disease model rats revealed irreversible binding and correlated with the presence of macrophages involved in the MI healing process [127].

### Physiological potency and GLP1R antagonists

Most commonly used GLP-1R targeting radioimaging agents are based on exendin-3 and exendin-4 peptides that present some issues such as high potency of the agonist inducing hypoglycemia [26, 66, 75]. In the case of potent ligands such as exendin-4 the amount that can be administered without induction of pharmacological effect can be very limited, however, if high amount of the peptide must be injected for various technical reasons, the episodes of severe hypoglycemia can be prevented by continuous infusion of glucose [38]. Another strategy to solve the problem of side effects is to use radiolabeled antagonists, and preclinical studies using agents based on exendin(9-39)-amide isolated from *Heloderma suspectum* venom have been conducted [67, 109, 128]. The GLP-1R targeting properties of  $^{125}\text{I}$ -Bolton-Hunter conjugated Ex(9-39)NH $_2$  ( $^{125}\text{I}$ -BH-exendin(9-39)) were confirmed both in vitro and in vivo in mouse [109]. Further investigation demonstrated that the number of binding sites was not higher for the antagonist  $^{125}\text{I}$ -BH-exendin(9-39) as compared to the agonist [111]. The authors also demonstrated the influence of the BH labeling site on the targeting properties, in particular, BH labeling on Lys $^{19}$  resulted in the agent with similar affinities to both rat and human GLP-1 receptors, while agent labeled at Lys $^4$  detected only rat GLP-1 receptors. Pharmacokinetics of  $^{125}\text{I}$ -BH-Ex(9-39)NH $_2$  studied in nude mice bearing rat Ins-1E tumors demonstrated low kidney uptake and fast blood clearance, however the uptake in tumor also decreased by 50% within 4 h [128]. Another antagonist analogue, [Lys $^{40}$ (DTPA- $^{111}\text{In}$ )]exendin(9-39), was compared to the agonist agents [Lys $^{40}$ (DTPA- $^{111}\text{In}$ )]exendin-3 and [Lys $^{40}$ (DTPA- $^{111}\text{In}$ )]exendin-4 [67]. All three agents exhibited similar IC $_{50}$  values in cell culture, however antagonist [Lys $^{40}$ (DTPA- $^{111}\text{In}$ )]exendin(9-39) demonstrated low specific uptake with fast washout in vivo in mouse xenografts. The introduction of chelator moiety at Lys $^{27}$  instead of Lys $^{40}$  did not improve the binding characteristics of antagonist [Lys $^{27}$ (Ahx-DOTA- $^{68}\text{Ga}$ )]Ex(9-39)NH $_2$  and [Lys $^{27}$ (NODAGA- $^{68}\text{Ga}$ )]Ex(9-39)NH $_2$  [128]. The authors found these

candidates not suitable for imaging of the GLP-1 receptor expression in vivo. Labeling with  $^{125}\text{I}$  of antagonist exendin(9-39) at terminal Tyr $^{40}$ , [Nle $^{14}$ , $^{125}\text{I}$ -Tyr $^{40}$ -NH $_2$ ]]Ex (9-39), also did not improve the tumor accumulation in mice despite recognition of larger number of binding sites [112]. The uptake in pancreatic beta cells and insulinomas was found species dependent for another antagonist,  $^{125}\text{I}$ -BH-exendin(9-39), in particular no binding was observed in human tissue [110]. Antagonist, [ $^{18}\text{F}$ ]FB40-Ex(9-39), visualized mouse pancreas within 30 min post injection with moderate pancreas-to-organ ratio [105].

### Kidney uptake reduction

The major difficulties of the accurate localization and quantification of the beta cells in vivo in rodents, in particular is the proximity to the left kidney and the irregular shape of the pancreas that cannot readily be accurately identified by CT. In the preclinical setup using mice and rats, nephrectomy provides the solution, even if this precludes longitudinal imaging also in animals, e.g. baseline and follow-up scans in treatment studies. The exploration of other options lead to the development of dual tracer methodology wherein additional agent with high accumulation in the exocrine pancreas and low kidney uptake is used for the accurate delineation of the pancreas [121]. In particular, the combination of [Lys $^{40}$ ( $^{111}\text{In}$ )DTPA]] exendin-3 and 2-[ $^{123}\text{I}$ ]Iodo-L-phenylalanine used in RIP-DTR mice demonstrated more accurate quantification of beta cells that correlated with ex vivo autoradiography results. In order to exclude necessity for the nephrectomy and additional probes, an image analysis method was developed and characterized [129]. The measurement of ROIs with 40% cutoff allowed reliable estimate of pancreatic uptake in vivo by SPECT/CT and  $^{111}\text{In}$ -labeled exendin-4 in mice [129].

The clinical relevance of the GLP-1R targeting radioactive agents might be hindered by the potential high radiation dose to the radiosensitive kidneys and the understanding of the uptake mechanism would allow development of means for the uptake reduction. Generally, peptides present renal excretion, and a common drawback of the metal radionuclide labeled exendin analogues used in the clinical studies is high kidney uptake. The high kidney uptake additionally presents a problem with respect to the imaging accuracy of adjacent pancreatic tail, especially in SPECT due to the intrinsically lower resolution in clinical scanners as compared to PET. It is essential to decrease the uptake not only for the accurate detection and quantification of the target of interest but also from the dosimetry and radiotherapeutic

point of view. The administered therapeutic radioactivity dose is very often limited by the renal retention and consequently high absorbed dose to the kidneys potentially could compromise kidney function. The high radiation dose may lead to renal failure and uremia. Mice receiving high kidney absorbed dose from  $^{111}\text{In}$ -DTPA-exendin-4 (>40 Gy) developed long-term kidney damage in tubular and glomerular compartments [130].

Although GLP-1R mRNA was identified in the kidneys previously [131], the uptake of  $^{111}\text{In}$ -DTPA-Lys<sup>40</sup>-exendin4 could not be precluded by excess of non-labeled ligand [62] and was higher compared to the radioiodinated analogues. The target accumulation of radioactivity using  $^{111}\text{In}$ -DTPA-Lys<sup>40</sup>-exendin-4 was found superior to radioiodinated peptides in terms of sensitivity and specificity [62]. Ex vivo autoradiography of rat kidney frozen sections using [ $^{177}\text{Lu}$ ]-DO3A-VS-Cys<sup>40</sup>-exendin-4 [59] revealed high uptake localized in the cortex indicating that most likely the radioactivity retention occurred due to tubular reabsorption of the peptide [132]. The renal function in rats was not compromised by acute administration of 50 MBq/kg [ $^{177}\text{Lu}$ ]-DO3A-VS-Cys<sup>40</sup>-exendin-4 according to the blood creatinine level. Despite the notion of GLP-1R expression in renal cortex, the uptake of [ $^{68}\text{Ga}$ ]-DO3A-VS-Cys<sup>40</sup>-exendin-4 could not be precluded by the excess of co-administered exendin-4 [26, 58]. More studies demonstrated that the vast majority of renal uptake was not GLP-1R mediated since it was not possible to block the uptake by the excess of unlabeled analogues [68, 86]. It is still possible that the kidneys present some GLP1R mediated binding of radiolabeled exendin-4, but this would be negligible in comparison to the uptake due to reabsorption according to the available literature.

Various agents partially precluding renal peptide reabsorption, e.g. arginine, lysine, gelofusine, and sodium maleate were suggested. The effect of *D*- and *L*-lysine on the renal uptake reduction was thoroughly investigated preclinically and clinically for antibodies and antibody fragments [133] indicating that the positively charged amino groups neutralize the negative charge of the luminal tubular cell surface thus precluding reabsorption of protein/peptide molecules. The co-administration of *L*-lysine and/or *L*-arginine became an integrated part of peptide receptor radionuclide therapy in neuroendocrine tumors [134]. However, in case of exendin analogues the results were not encouraging most probably due to the negative charge of the exendin-3 peptide moiety [135].

Preclinical studies have been conducted to investigate the kidney uptake mechanism, and

megalyn mediated reabsorption mechanism in combination with metabolic trapping was hypothesized [62]. A natural megalyn ligand, albumin and its fragments were investigated precluding the uptake of  $^{111}\text{In}$ -exendin in rat kidneys by 52% wherein lysine and gelofusine reduced the kidney uptake, respectively by 15 and 25% [136]. Furthermore, in vivo studies using megalin-deficient mice demonstrated lower kidney uptake of  $^{111}\text{In}$ -DTPA-exendin-3 analogue compared to wild-type mice indicating binding to megalin receptor with subsequent internalization and lysosomal entrapment as the mechanism of kidney uptake and retention [135]. The extent of the uptake reduction was different for male and female mice with respective values of 62% and 52%, and interestingly it was also dependent on the administered peptide mass with higher reduction values for the higher peptide doses presumably indicating higher specificity of the agent towards megalin receptors. Repeated administered dose of 40-50 MBq of  $^{111}\text{In}$ -DTPA-exendin-4 resulted in 70 Gy kidney absorbed dose in wild-type mice while in megalin-deficient mice was it 20-40 Gy [130].

It was hypothesized that the renal reabsorption is influenced by the number of charged amino acids and their distribution over the peptide chain [137]. Kidney uptake of [ $\text{Lys}^{40}(\text{Ahx-DO3A-}^{68}\text{Ga})\text{NH}_2$ ]-exendin-4 was reduced by pretreatment with positively charged poly-glutamic acid (PGA, 49%) or the plasma expander Gelofusine (succinylated gelatin, 60%). A combination of PGA and Gelofusine decreased the renal uptake even further (78%) [69, 137]. The kidney uptake of  $^{111}\text{In}$ -DTPA-Lys<sup>40</sup>-exendin-4 in rats was also reduced by either PGA (29%) or Gelofusine (19%) used separately, however their synergetic effect was the highest causing 48% uptake reduction [137]. Interestingly, anionic amino acid Lysine did not affect the kidney uptake in rat, indicating that exendin-4 is taken up in the kidneys by a mechanism different from that of somatostatin analogues. The promising preclinical results on renal uptake reduction using plasma expanders was recently partly confirmed in a clinical study in healthy volunteers, where gelofusine reduced the renal uptake of  $^{111}\text{In}$ -DTPA-Lys<sup>40</sup>-exendin-4 by almost 20%, while not impacting the pancreatic binding [138]. Thus, interpolating these results to exendin-4 peptide receptor radionuclide therapy (PRRT) using lutetium-177 as label, the authors estimate that the amount of  $^{177}\text{Lu}$ -exendin-4 could be increased accordingly without reaching the 23Gy limit in kidney. In a simulation, insulinomas could be exposed to up to 156 Gy which is in range for doses inducing tumor shrinkage by DOTATATE PRRT.

Furthermore, the intervention improved delineation of the pancreatic tail allowing improved assessment of GLP1R density.

The hypothesis of the involvement of megalin and cubilin receptors in the renal reabsorption was tested by using derivatives of albumin, a natural ligand to megalin and cubilin receptors [136, 139]. Fragments of albumin, derived from the digestion of albumin by cyanogen bromide, with various charges were studied. The biodistribution of the fragment of 36 AA and -3 net charge in rats demonstrated inhibition of [Lys<sup>40</sup>(Ahx-DTPA-<sup>111</sup>In)NH<sub>2</sub>]-exendin-3 reabsorption by 26% with no effect on any other organ uptake, and no adverse effects.

The kidney retention is influenced by the radionuclide labeling chemistry and the difference in the physicochemical properties of the radiolabeled catabolites. For example, lysosomal degradation of a protein/peptide radioiodinated directly at tyrosine yields lipophilic catabolites of iodinated tyrosine that leave the tubule cell. While degradation of proteins/peptides either radioiodinated via prosthetic groups or radiometalated via chelator moiety results in hydrophilic and charged radioactive catabolites that get trapped inside the cell. The feasibility of tuning of kidney uptake by using halogen radiolabels has been studied. The kidney uptake decrease could also be achieved using Ex(9-39)NH<sub>2</sub> antagonist analogues labeled with non-residualizing <sup>125</sup>I moiety [128, 140] and <sup>18</sup>F [74, 81]. Exendin-4 analogue labeled with <sup>125</sup>I via tyrosine residue was reported to drastically decrease the kidney uptake to only 7.5±0.7%IA/g [112] or 3.3±0.6%IA/g [141]. The ratio of tumor-to-kidney investigated in mice with insulinoma cell xenografts was 50 times higher for [Nle<sup>14</sup>,<sup>125</sup>I-Tyr<sup>40</sup>-NH<sub>2</sub>]exendin-4 (9.7) as compared to [Nle<sup>14</sup>,Lys<sup>40</sup>(Ahx-DOTA-<sup>68</sup>Ga)-NH<sub>2</sub>]exendin-4 (0.2). However, protection of thyroid was required, and was reduced by 94% using irenat. The authors attributed the low kidney retention to the *in vivo* deiodination of the agents. The improvement of tumor-to-kidney ratio for <sup>125</sup>I-BH-Ex(9-39)NH<sub>2</sub> was 20-fold as compared to [Nle<sup>14</sup>, Lys<sup>40</sup>(Ahx-DOTA-<sup>68</sup>Ga)NH<sub>2</sub>]Ex-4 [128]. The drawback of using <sup>125</sup>I-BH-Ex(9-39)NH<sub>2</sub> was high accumulation in the thyroid, however it could be considerably reduced by inhibitor of the sodium iodide symporter (e.g. irenat) [142, 143]. Exendin-4 labeled with <sup>18</sup>F (<sup>18</sup>F-TTCO-Cys<sup>40</sup>-exendin-4) demonstrated considerably lower kidney uptake as compared to radiometal-labeled counterparts [84]. The fast renal clearance was also demonstrated for another <sup>18</sup>F-labeled analogue, [Nle<sup>14</sup>,Lys<sup>40</sup>]-[<sup>18</sup>F]exendin-4 [108]. Silicon containing exendin-4 labeled with <sup>18</sup>F [104] and antagonist, [<sup>18</sup>F]FB40-Ex(9-39) [105] also demonstrated lower

kidney uptake and retention comparable to radiometal labeled agents. On the other hand, it should also be noted that the uptake in GLP-1R rich target tissues (e.g. pancreas or insulinoma) of radio-halogenated exendin analogues may similarly be decreased by the lack of a radionuclide trapping mechanism.

Another possible reason for the high kidney uptake is the metabolism of the exendin analogues, and final elimination of the catabolites by kidney [144]. Improved stability of exendin-based agents could potentially decrease the kidney uptake and absorbed dose. It was demonstrated in pigs that the degradation of GLP-1 was influenced by NEP, and inhibition of NEP and dipeptidyl peptidase IV (DPPIV) *in vivo* could improve metabolic stability of the ligand [145]. However, the improvement could be predicted to be minor, given that one of the primary reasons for the development of exendin-4 as a therapeutic GLP-1R agonist, was its resistance to DPPIV as compared to endogenous GLP-1.

An alternative approach was to introduce a metabolizable linkage Nε-maleoyl-L-lysyl-glycine (MAL) into an exendin-4 analogue ([<sup>64</sup>Cu]NODAGA-MAL-exendin-4) [99]. The novel agent maintained the biological activity and demonstrated specific uptake in rat pancreatic islets, however kidney uptake was not reduced compared to [<sup>64</sup>Cu]NODAGA-exendin-4 without the linkage. A cleavable substrate for meprin β protease expressed in the kidney brush-border membrane was introduced between the binding moiety of exendin-4 and <sup>111</sup>In-NODAGA moiety [146]. The biodistribution in nude mice bearing CHL-GLP-1R positive xenografts showed specific accumulation in the tumor cells despite the introduced modification. Recombinant meprin β efficiently digested the linker sequence in *in vitro* assay. However, the kidney uptake *in vivo* was comparable to that of the reference agent, <sup>111</sup>In-NODAGA-exendin-4. The authors hypothesized that the peptide uptake was most probably faster than the cleavage of the linker.

<sup>68</sup>Ga-NOTA-MVK-Cys<sup>40</sup>-Leu<sup>14</sup>-exendin-4 comprising cleavable Met-Val-Lys (MVK) sequence demonstrated remarkable reduction in kidney uptake compared to <sup>68</sup>Ga-NOTA-Cys<sup>40</sup>-Leu<sup>14</sup>-exendin-4 while retaining high accumulation in GLP-1R expressing INS-1 mouse xenografts (Figure 4) [98]. Presumably, the agent was cleaved by brush border membrane enzyme on kidneys to <sup>68</sup>Ga-NOTA-Met-OH that was rapidly excreted.

## Clinical accomplishments

A number of clinical research studies has been performed since the first study on two patients with

insulinoma using  $[Lys^{40}(Ahx-DTPA-^{111}In)NH_2]$ -exendin-4 (DTPA: diethylenetriamine tetraacetic acid) for the imaging of GLP-1R [64] and nowadays several multicenter clinical trials using various GLP-1 analogues are ongoing in Europe [26, 37, 64-66, 147-149]. Exendin-4 analogues that are relatively stable agonists of GLP-1R labeled with gamma emitting radionuclides such as  $^{111}In$  and  $^{99m}Tc$  demonstrated high sensitivity in GLP-1R imaging and insulinoma detection with SPECT [65, 66, 150]. PET technique offers further advantages of higher sensitivity and spatial resolution as well as accurate quantification. These advantages are crucial especially considering the small size of insulinomas. Such positron emitting radionuclides as  $^{18}F$ ,  $^{64}Cu$ ,  $^{68}Ga$ , and  $^{89}Zr$  have been used offering both advantages and drawbacks of their physical and chemical characteristics.

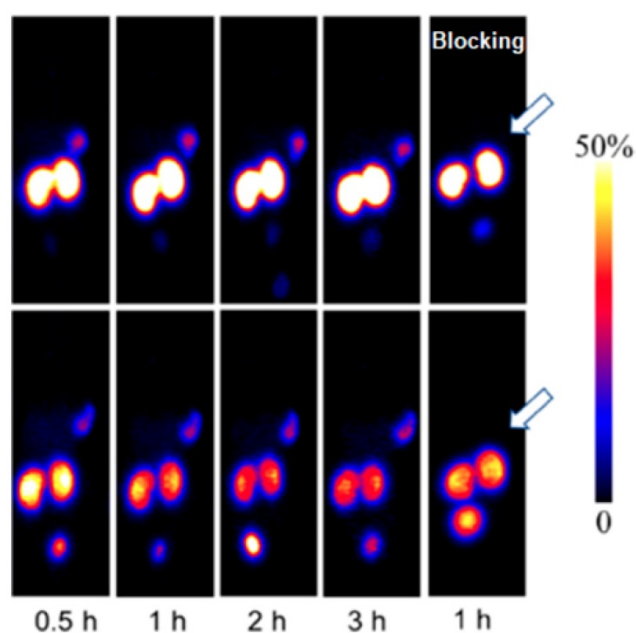


**Figure 4.** MicroPET images of INS-1 tumor mice at different time points after intravenous injection of  $^{68}Ga$ -NOTA-Cys<sup>40</sup>-Leu<sup>14</sup>-exendin-4 (upper panel) and  $^{68}Ga$ -NOTA-MVK-Cys<sup>40</sup>-Leu<sup>14</sup>-exendin-4 (lower panel). Reproduced from [98].

## SPECT/CT

Exendin-4 ligand modified with either DTPA or DOTA at lysine amino acid residue and labeled with  $^{111}In$  resulting in  $[Lys^{40}-(Ahx-DTPA-^{111}In)NH_2]$ -exendin-4 and  $[Lys^{40}-(Ahx-DOTA-^{111}In)NH_2]$ -exendin-4 demonstrated prominent detection of insulinomas that could not be unambiguously localized by conventional radiological methods [64, 66]. The localization of the lesion enabled successful guided surgery in both patients [64], and the delineation of benign insulinomas was accomplished in six patients [66] wherein morphological diagnostic

methods were conclusive in four out of six cases. Moreover, the long physical half-life of  $^{111}In$  allowed the subsequent resection of the tumor mass by radioguided surgery using  $\gamma$ -probe intraoperatively [66]. The overexpression of GLP-1R in the resected lesion tissue was confirmed by vitro autoradiography. The potential of  $[Lys^{40}-(Ahx-DTPA-^{111}In)NH_2]$ -exendin-4 SPECT/CT for the improved patient management was investigated in a prospective study with 11 patients affected by malignant insulinoma [37]. The patients were also examined with  $^{68}Ga$ -DOTATATE PET/CT for the detection of SSTR expressed in high density in malignant insulinoma. The authors concluded that in contrast to benign insulinomas, malignant insulinomas often lack GLP-1 receptors while express SSTR type 2 more often. A subsequent larger study with 30 patients demonstrated that  $[Lys^{40}-(Ahx-DTPA-^{111}In)NH_2]$ -exendin-4 SPECT/CT was more sensitive diagnostic technique than conventional CT/MRI in detection of insulinomas and it changed therapeutic management of patients affected by endogenous hyperinsulinaemic hypoglycemia [150]. These successful studies also pointed out the limitation of the low spatial resolution of  $^{111}In$ /SPECT and interference of the high kidney uptake with detection of lesions in pancreas regions close to the kidney. The adequate localization required a second SPECT examination 3-7 days later after the sufficient clearance of the kidneys from the radioactivity.

Five healthy volunteers and five patients affected by T1D were engaged in a study using  $^{111}In$ -DTPA-exendin wherein significant reduction (60%) of the integrated radioactivity uptake in the pancreas (i.e. radioactivity concentration multiplied with pancreas volume) was observed in the patients [57]. Despite high interindividual variation, the separation of the two groups was distinguishable. However, the radioactivity concentration of  $^{111}In$ -DTPA-exendin in the pancreas was overlapping between the healthy controls and the subjects with T1D, suggesting that the atrophy of the pancreas in long standing T1D accounted for the majority of the decreased integrated uptake [54]. Further, these results indicate binding of  $^{111}In$ -DTPA-exendin in the pancreas of subjects with T1D in the range of the healthy controls. This surprising finding was suggested to indicate evidence of a population of residual GLP-1R expressing beta cells long after T1D debut. Another source of the signal may occur from binding of  $^{111}In$ -DTPA-exendin to other GLP-1R positive cell types in the pancreas, which has been shown to vary considerably between species [46]. These and other outstanding questions are addressed by an ongoing clinical trial where  $^{111}In$ -DTPA-exendin

is administered prior to planned removal of part of the pancreas, where the autoradiographic uptake pattern in pancreatic sections will be correlated to the islet distribution (NCT03889496). The reduction of kidney uptake of  $^{111}\text{In}$ -DTPA-Lys<sup>40</sup>-exendin-4 by 18.1% was achieved in a clinical study with ten healthy volunteers using Gelofusine [138]. The procedure even allowed for better discrimination of the pancreatic tail without reduction of the pancreatic uptake. Importantly, in relation to potential radiotherapy applications, the procedure yielded an improved dosimetric profile. Exendin-4 based imaging in metabolic disease has otherwise shifted towards  $^{68}\text{Ga}$  based-PET imaging, which is outlined in detail below.

The lower  $\gamma$ -energy and shorter half-life of  $^{99\text{m}}\text{Tc}$  as compared to  $^{111}\text{In}$  could improve the quality of images and considerably reduce the radiation burden to the patient and medical staff. The ready availability of  $^{99\text{m}}\text{Tc}$  from a generator system provides another crucial advantage. The respective agent, [Lys<sup>40</sup>(Ahx-HYNIC- $^{99\text{m}}\text{Tc}$ /EDDA)NH<sub>2</sub>]exendin-4, was used in a study of 11 patients with negative results on conventional diagnostic imaging methods [65]. The sensitivity and specificity of [Lys<sup>40</sup>(Ahx-HYNIC- $^{99\text{m}}\text{Tc}$ /EDDA)NH<sub>2</sub>]exendin-4 SPECT/CT were assessed to be 100% in patients with benign insulinoma. In one patient out of two with malignant insulinoma the lesion was found only in the region of local recurrence. In the subsequent study [39] forty patients with hypoglycemia were examined with [Lys<sup>40</sup>(Ahx-HYNIC- $^{99\text{m}}\text{Tc}$ /EDDA)NH<sub>2</sub>]exendin-4 SPECT/CT and positive results were observed in 28 patients. The high kidney uptake presented similar complications as in the case of  $^{111}\text{In}$ -labeled analogues and the optimal imaging time in terms of pancreatic lesion localization was determined as 5–6 h post injection. [Lys<sup>40</sup>(Ahx-HYNIC- $^{99\text{m}}\text{Tc}$ /EDDA)NH<sub>2</sub>]exendin-4 SPECT/CT was also successfully used for the diagnostic detection of medullary thyroid cancer [151].

## PET/CT

Clinical PET scanners offer advantages over SPECT in terms of higher spatial resolution and sensitivity, accurate quantification of the tracer uptake and consequently target concentration as well as possibility for dynamic scanning and subsequent kinetic modeling and uptake mechanism investigation. Digital detectors introduced to the new generation of PET/CT and PET/MRI scanners increase the throughput, improve sensitivity and resolution making the PET technique even more attractive. Positron emitting  $^{68}\text{Ga}$  is a very attractive radionuclide in terms of its ready availability from a

simple generator system as well as cyclotron, straightforward labeling chemistry, and favorable decay characteristics [117]. In the context of theranostics,  $^{68}\text{Ga}$  is particularly interesting, as it forms a diagnostic/therapeutic radionuclide pairing with  $^{177}\text{Lu}$ , with which it shares critical features such as the ability to form stable complex with DOTA.

The development and clinical introduction of  $^{68}\text{Ga}$  is accelerating [117] and  $^{68}\text{Ga}$  has been employed to label several exendin-4 analogues. The uptake of the radiopharmaceuticals could be localized with high contrast in pancreas and insulinoma lesions. A case examination of a patient with severe hypoglycemia was conducted using an [ $^{68}\text{Ga}$ ]Ga-DO3A-VS-Cys<sup>40</sup>-Exendin-4 PET/CT [26]. Multiple small liver metastases and paraaortal lymph node lesions were clearly visualized (Figure 5), while computed tomography, ultrasound, [ $^{18}\text{F}$ ]Fluorodeoxyglucose/PET-CT or [ $^{11}\text{C}$ ] 5-Hydroxytryptophan/PET-CT could not provide conclusive results. [ $^{68}\text{Ga}$ ]Ga-DO3A-Exendin-4/PET-CT examination impacted the treatment of the patient and thus demonstrated its potential for the management of this disease [26]. Clinical study where 5 patients with endogenous hyperinsulemic hypoglycemia were enrolled was conducted [87]. [Nle<sup>14</sup>,Lys<sup>40</sup>(Ahx-DOTA- $^{111}\text{In}$ )NH<sub>2</sub>]exendin-4 and [Nle<sup>14</sup>,Lys<sup>40</sup>(Ahx-DOTA- $^{68}\text{Ga}$ )NH<sub>2</sub>]exendin-4 [87] were compared in terms of detection rate, resolution, and background uptake. [Nle<sup>14</sup>,Lys<sup>40</sup>(Ahx-DOTA- $^{68}\text{Ga}$ )NH<sub>2</sub>]exendin-4 correctly identified the insulinoma in 4 of 4 patients, whereas [Nle<sup>14</sup>,Lys<sup>40</sup>(Ahx-DOTA- $^{111}\text{In}$ )NH<sub>2</sub>]exendin-4 SPECT/CT correctly identified the insulinoma in 2 of 4 patients. [Nle<sup>14</sup>,Lys<sup>40</sup>(Ahx-DOTA- $^{68}\text{Ga}$ )NH<sub>2</sub>]exendin-4 was shown to be sensitive in localizing hidden benign insulinomas and was found superior in terms of shorter examination time, higher tumor-to-background ratio, higher spatial resolution, lower radiation dose, and accurate quantification.

The detection of occult insulinoma was enabled by  $^{68}\text{Ga}$ -NOTA-MAL-Cys<sup>40</sup>-exendin-4 PET/CT and subsequent surgical removal of the pancreas tail insulinoma resulted in recovery from hypoglycemia [75]. The imaging was performed 2 h post injection in order to decrease the kidney uptake and allow visualization of the pancreas tail. In the subsequent prospective study, the authors explored the potential of  $^{68}\text{Ga}$ -NOTA-exendin-4 PET/CT for the detection of insulinomas in a larger patient cohort and found sensitivity in the localizing of the lesions of 97.7% which was considerably higher than that of CT (74.4%), MRI (56.0%), EUS (84.0%), and  $^{99\text{m}}\text{Tc}$ -HYNIC-TOC (19.5%) (Figure 6) [38]. Lesions as small as less than 1.0 cm were detected by  $^{68}\text{Ga}$ -NOTA-MAL-Cys<sup>40</sup>-exendin-4 PET/CT in 11

patients. The kidney uptake was high interfering with the detection of pancreas tail lesions, however additional examination 2-3 h post injection resulted in unambiguous delineation. Noteworthy, the only patient diagnosed with malignant insulinoma showed high uptake in both  $^{68}\text{Ga}$ -NOTA-MAL-Cys<sup>40</sup>-exendin-4 PET/CT and  $^{99\text{m}}\text{Tc}$ -HYNIC-TOC. [Lys<sup>40</sup>-(Ahx-DOTA- $^{68}\text{Ga}$ )NH<sub>2</sub>] PET/CT clearly delineated pancreatic lesion while [Lys<sup>40</sup>-(Ahx-DOTA- $^{111}\text{In}$ )NH<sub>2</sub>] SPECT/CT was not conclusive in an inpatient comparative study [76]. The high GLP-1R expression was confirmed on the tissue after the pancreatectomy that resolved the hypoglycemia. The density of GLP-1R was 3-fold higher in the islets of this nesidioblastosis patient as compared to that of normal pancreas islets implying that [Lys<sup>40</sup>-(Ahx-DOTA- $^{68}\text{Ga}$ )NH<sub>2</sub>] PET/CT may be a valuable tool in determining the surgical strategy also in nesidioblastosis which can be a focal disease. A lesion located at the proximal jejunum, below the body of pancreas and multiple liver metastases were clearly detected by  $^{68}\text{Ga}$ -exendin-4 PET/CT enabling efficient treatment of the patient [152].  $^{68}\text{Ga}$ -DOTA-exendin PET/CT aided conclusive diagnosis accurately localizing the culprit lesion for the subsequent surgery [153]. The patient experienced complete postoperative recovery.  $^{68}\text{Ga}$ -DOTA-exendin PET/CT was the only method that could visualize the pancreatic lesion and thus facilitate curative surgical treatment [154, 155]. Detection of an insulinoma lesion using  $^{68}\text{Ga}$ -DOTA-exendin PET/CT enabled subsequent ultrasound-guided ethanol ablation and monitoring of the tumor response to the treatment [156]. A large multicenter study comparing  $^{68}\text{Ga}$ -NODAGA-exendin-4 with  $^{68}\text{Ga}$ -DOTATATE in 56 subjects with adult hyperinsulinemic hypoglycemia is ongoing (ClinicalTrials.gov identifier: NCT03189953) and is expected to clarify the role of  $^{68}\text{Ga}$  labeled exendin-4 in the management of this group of diseases including insulinoma.

GLP-1R imaging has potential in metabolic disease in human given its expression in human pancreatic islets and the incretin effect. Thus, there are several clinical trials ongoing that aim to elucidate the impact of  $^{68}\text{Ga}$ -exendin-4 PET imaging in different aspects of metabolic disease. Hitherto, clinical results on  $^{68}\text{Ga}$ -exendin-4 PET have not yet been published in journal format, thus this is an overview of studies published in international trial database (clinicaltrial.gov). The GLP-1R expression in pancreas (assumed to be correlated to the beta cell mass) is investigated by  $^{68}\text{Ga}$ -NODAGA-exendin-4 PET/CT in T1D subjects with unstable and stable glycaemic control (NCT03785275) as well as during the

honeymoon phase in T1D (NCT03917238) and in subject with gestational diabetes (NCT03182296). Furthermore, the possibility to detect functional islets in the liver of T1D subjects with intraportally transplanted islets is also evaluated (NCT03785236).

GLP-1R expression is also evaluated in subjects with T2D undergoing gastric bypass (NCT02542059). Finally, the value of  $^{68}\text{Ga}$ -NODAGA-exendin-4 in management of congenital hyperinsulinism in comparison with  $^{18}\text{F}$ -DOPA and contrast enhanced CT (NCT03768518) is under investigation. The results of the abovementioned studies are expected to improve the understating of GLP-1R expression in health and disease, as well as the notion of using  $^{68}\text{Ga}$ -exendin4 as a marker for beta cell mass.

### Side effects

In a preclinical PET imaging study with [ $^{68}\text{Ga}$ ]Ga-DO3A-VS-Cys<sup>40</sup>-exendin-4, pigs developed tachycardia after intravenous administration [94, 96], however to the best of our knowledge the published patient studies did not present such adverse effects. In some patients, transient palpitation at the time of injection that lasted a few seconds has been reported [38]. Slight plasma glucose concentration reduction but no severe hypoglycemic episodes were observed in a study of 6 patients with endogenous hyperinsulinemic hypoglycemia [66]. One patient experienced a short episode of vomiting, which may be expected at high doses of GLP-1 agonist being known to affect appetite and nausea. Moreover, clinical studies on the treatment of T2D patients with exenatide (synthetic exendin-4) over twelve weeks did not demonstrate clinically meaningful effects on heart rate [157] even though GLP-1R is expressed in heart [158].

### Intraoperative application

Another application elevating success of a surgery is intraoperative use of gamma-probe detecting  $^{111}\text{In}$ -DOTA-exendin-4 accumulated in the lesions [66, 159]. The method offers crucial advantage over intraoperative venous sampling which is a complex procedure with potential complications [36]. Fluorescent exendin probes could similarly accumulate in insulinoma lesions, and potentially offer improved resolution and delineation of tumors during removal compared to long-lived SPECT radionuclides. The combination of radionuclide and fluorescently labeled GLP-1R targeting probes potentially offers advantage of first localizing the tumor by whole body PET/SPECT imaging, followed by using the fluorescent signal for guiding accurate tumor removal [101].

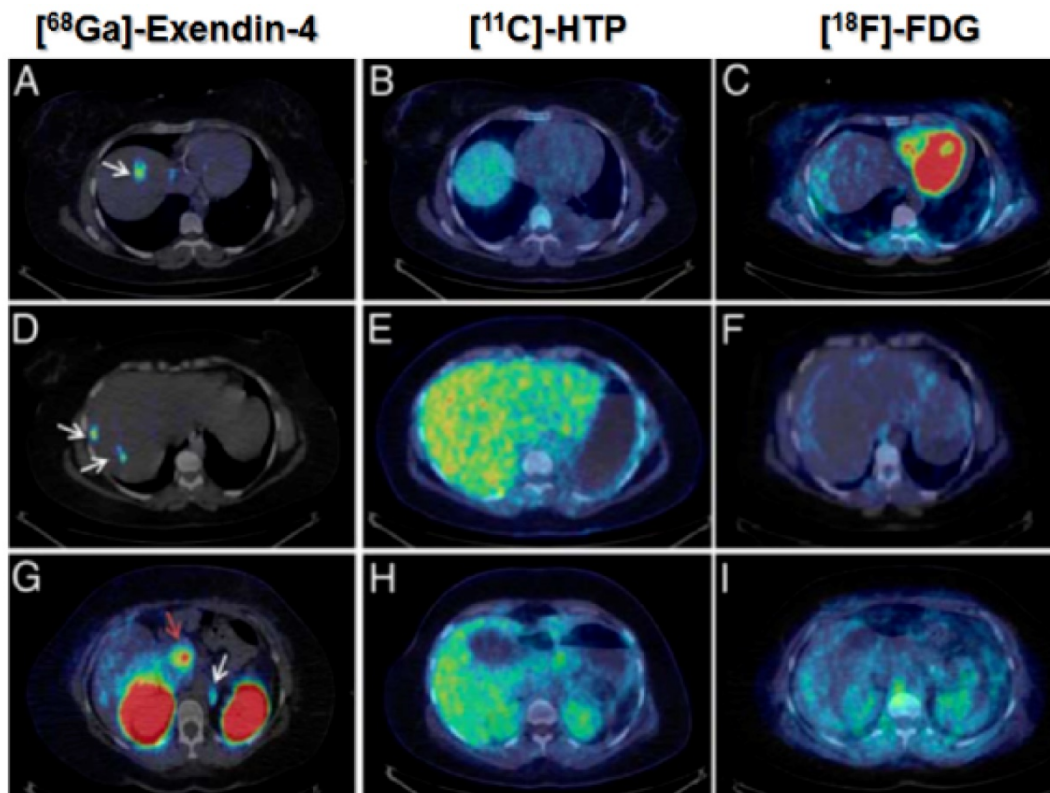


**Figure 5.** [<sup>68</sup>Ga]Ga-DO3A-Exendin-4/PET-CT revealed several GLP-1R positive lesions (white arrows) in the liver (A, D) and a paraaortic lymph node (G). Beta cells in normal pancreas (red arrow) have significant expression of GLP-1R and can also be visualized by this technique (G). No pancreatic or hepatic lesions could be detected by PET/CT using established tumor markers such as [<sup>11</sup>C]HTP (B, E, H) and [<sup>18</sup>F]FDG (C, F, I). Reproduced from [26].

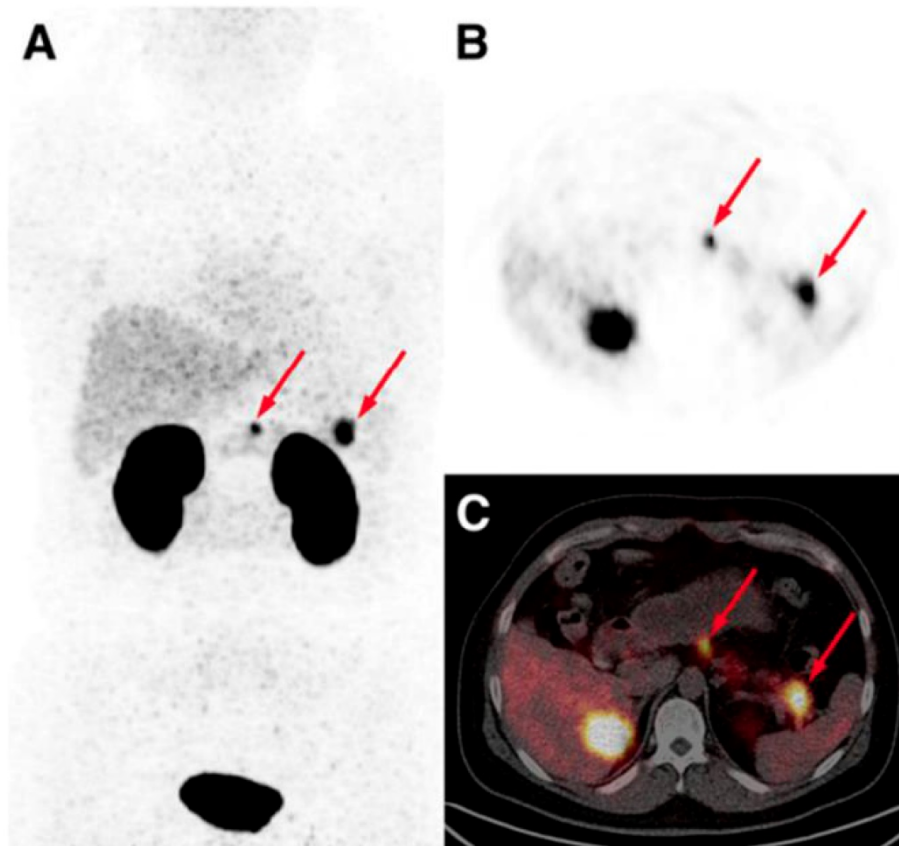


**Figure 6.** Maximum intensity projection (A) and axial PET (B) and PET/CT (C) images obtained from a patient 40 min post administration of <sup>68</sup>Ga-NOTA-exendin-4. Arrows point at two lesions in neck and tail of pancreas that were surgically removed and confirmed to be insulinomas histologically. Reproduced from [38].

## Theranostics/Radiotheranostics in GLP-1R targeting

Non-invasive imaging targeting GLP-1R can be used for the selection of treatment, monitoring treatment response, dose planning for the treatment based on both radioactive (radiotheranostics) and non-radioactive (theranostics) pharmaceuticals [160]. It is a promising tool in both diabetes and cancer.

### Theranostics in diabetes

GLP-1 analogues are of strong interest in the context of theranostics since the treatment of the diabetes is also targeted at GLP-1R (the broad class of GLP-1 agonists) and thus the drug efficacy and dose can potentially be predicted and planned individually and the patient response to the drug can be monitored enabling adjustment of the treatment respectively. Little is known of the numerical variation of GLP-1R expression in the human pancreas, but initial data from imaging studies with radiolabeled exendin-4 indicates significant variation in individuals. This observation combined with the notion that some patients develop tolerance to GLP-1 agonists indicate a potential area of application for exendin-4 based imaging.

Quantitative GLP-1R imaging has been proposed for the assessment of drug mediated occupancy in the pancreas both preclinically and clinically. This could theoretically be used to benchmark different GLP-1 agonists versus each other, as well as assist in improving understanding of the dose-effect relationship. This is particularly important for GLP-1R agonist since there is likely an optimal dosing and exposure interval with adequate clinical efficiency, while doses exceeding this may induce side effects, e.g. nausea.

The in vivo monitoring and quantification of the endogenous and transplanted beta cells would provide crucial information on the cell survival and the loss of functionality. Prospective in vivo studies for the measurement of beta cell mass in diabetic patients and healthy individuals would potentially allow understanding of underlying disease mechanisms and assignment of individualized treatments. Stratification of patients depending on levels of functional beta cells in pancreas may even impact the diagnosis, as the current major classifications of diabetes (T1D, T2D, gestational diabetes) may be too simplified and do not accurately describe the underlying disease progression [161, 162]. Novel sub-categories of diabetes have been proposed based on phenotypical and metabolic characteristics. Furthermore, it is expected that novel imaging techniques for BCM quantification could

contribute to such phenotypic characterization in the future.

The abovementioned predictive theranostic applications require precise, non-invasive, quantitative method that would allow repetitive examinations as potentially subtle changes or differences in GLP-1R expression or BCM must be detected and quantified. Broader deployment of exendin-4 mediated GLP-1R PET scanning in the clinic for theranostic studies (outside of insulinoma management) as described above is based on the availability of some crucial data. Some of the data is expected to be available based on the outcome of already ongoing clinical trials. Current preclinical data clearly support the notion that the GLP-1R expression can be quantified in the pancreas with high precision by PET, but this precision must be verified in clinical PET studies (see for example ongoing study NCT03350191). Additionally,  $^{68}\text{Ga}$ -exendin-4 PET outcome is currently usually reported as SUV uptake in pancreas at certain time points (often some interval between 50-90 minutes after administration). This semi-quantitative assessment has never been benchmarked against a full kinetic model including arterial input corrected for metabolic stability of the radioligand. Such a comparison would reduce the ambiguity of the semi-quantitative endpoint and instead objectively point to a time-point and scanning duration were the SUV measurement correlates with the golden standard PET model assessment. Furthermore, such validation would remove the future need of including venous or arterial sampling (i.e. reduce the invasiveness of the procedure) as well as replacing the need for dynamic scanning with a static pancreatic scan of shorter duration (i.e. improve patient comfort and examination throughput). Again, also these outstanding questions may be answered by the outcome of NCT03350191. Finally, the notion of  $^{68}\text{Ga}$ -exendin-4 as a surrogate marker for human pancreatic BCM is dependent on the outcome of study NCT03889496 that will verify the important islet-to-exocrine binding ratio of radiolabeled exendin-4 by post resection autoradiography of the pancreas in human.

The long-term outcome of several clinical studies on intraportal islet transplantation, including the Edmonton protocol [8] have demonstrated that monitoring of transplanted islets in vivo is crucial for assessing the efficacy of different transplantation procedures. PET imaging of prelabeled islets demonstrated significant islet loss during the acute peri-transplant phase [163], but longitudinal repeatable and direct assessment of engrafted viable islet mass are lacking in the clinic. Healthy islets were isolated from the pancreas of a patient that underwent

insulinoma surgery and were re-implanted into brachioradialis muscle [10]. The beta cells could successfully be visualized in vivo using  $[Lys^{40}(Ahx-DTPA-^{111}In)NH_2]$ exendin-4 one year after the transplantation. High interindividual variation was observed in patients affected by T1D [57] indicating that the individual approach to the treatment regimen is required to monitor response and adjust the dose or alter the medication for the improved treatment outcome. Moreover, a substantial variation in beta cell mass is found also amongst healthy subjects [55].

### Radiotheranostics in cancer

Radiotheranostics for the management of neuroendocrine patients is the most prominent and pioneer example. The radionuclide  $^{68}Ga$  and  $^{177}Lu$  pair is the most frequently used one in the context of PRRT. Both Ga(III) and Lu(III) form stable complexes with DOTA chelator conjugated to somatostatin analogues, in most cases allowing for the use of the same ligand molecule to assure the least variation in the biodistribution pattern. The investigation of the feasibility of the similar approach for ligands targeting GLP-1, CCK, and GIP receptors is of utmost interest [164]. The radiotherapeutic effect of  $[Lys^{40}(Ahx-DTPA-^{111}In)NH_2]$ -exendin-4 was demonstrated in mice with Rip1Tag2 spontaneous insulinoma [88]. The tumor reduction was observed in radioactivity dose dependent manner by up to 94%. The therapeutic effect was assigned to tumor cell apoptosis, necrosis, and decreased proliferation.

### Dosimetry and feasibility of radiotheranostics

Pre-therapeutic imaging in the context of internal targeted radiotherapy has two major objectives: 1. Dosimetry investigation wherein radiation absorbed dose to healthy organs is measured to assess the potential radiotoxicity; 2. Estimation and planning of radiation dose that would provide effective radiotherapy on one hand and safe radiation dose to the healthy organs on the other hand. Dosimetry investigation plays a crucial role in the radiopharmaceutical development in terms of estimating the number of annual examinations that can be conducted without presenting hazard to normal organs as well as in the context of internal radiotheranostics. The major factors that influence the radiation dose is the biodistribution, excretion, and radionuclide decay characteristics such as half-life and radiation type.

High kidney uptake with subsequent high radiation dose is the major factor precluding the radiotherapeutic use of exendin-based analogues labeled, e.g. with  $^{111}In$  and  $^{177}Lu$  [26, 59, 66, 75, 88]. For

example,  $[Lys^{40}(Ahx-DTPA-^{111}In)NH_2]$ -exendin-4 accumulated in kidneys with high absorbed radiation dose caused morphological changes thus hindering radiotherapeutic application of  $^{111}In$ . However, it should be mentioned that  $^{177}Lu$  is more efficient than  $^{111}In$  as experience with somatostatin radiotherapy indicates. Lower kidney uptake observed for the iodine-based analogues would present an advantage from the radiotheranostic point of view with positron emitting  $^{124}I$  and radiotherapeutic  $^{131}I$  [160]. However, initial results of such analogues demonstrated fast washout of  $^{125}I$ -BH-Ex(9-39) $NH_2$  radioactivity from mouse xenograft [128] and therapeutic outcome using respective  $^{131}I$  labeled analog has not been demonstrated. Additional advantage of using  $^{123}I$ ,  $^{124}I$ / $^{131}I$  imaging/radiotherapeutic pair would be the identical chemical structure of the radiopharmaceuticals providing identical biodistribution pattern.

The physiological expression of GPL-1R in the endocrine pancreas, intestine, lung, kidney, breast and brain potentially may cause difficulty due to interference of the respective background uptake with the target uptake and radiation dose to those healthy organs. However, it should be mentioned that the clearance from blood and healthy organs without GLP-1R expression for the majority of exendin analogues is fast, and it does not impose dosimetry issues with  $^{68}Ga$ ,  $^{99m}Tc$ , or  $^{177}Lu$  [59, 86]. This is a very crucial factor with respect to radiation sensitive organ such as red marrow. Other organs with relevant expression of GLP-1R could conceivably exhibit significant binding of radiolabeled exendin and in turn deposit a high absorbed dose in surrounding tissues. However, the dosimetry in lung for example, with relevant physiological GLP-1R expression, has been shown to pose no concerns with regards to radiation safety [26, 58, 70]. Moreover, human lung express GLP-1R to lesser extent [32] as compared to rodents that the preclinical experiments were conducted with. The uptake of radiolabeled exendin analogues in the lung can be attributed not only to the presence of GLP-1R [68], but also megalin receptors as it was demonstrated in megalin-deficient mice [135].

Lower radiation burden from  $^{68}Ga$ -labeled analogues as compared to  $^{64}Cu$  [78] and  $^{111}In$  [69] labeled counterparts was demonstrated pre-clinically. Effective dose for  $[Lys^{40}(Ahx-NODAGA-^{68}Ga)NH_2, Nle^{14}]$ -exendin-4 was 12-fold lower than that for  $[Lys^{40}(Ahx-NODAGA-^{64}Cu)NH_2, Nle^{14}]$ -exendin-4 [78]. A comparative study of  $[Lys^{40}(Ahx-DOTA-^{111}In)NH_2]$ -exendin-4,  $[Lys^{40}(Ahx-DOTA-^{68}Ga)NH_2]$ -exendin-4, and  $[Lys^{40}(Ahx-hydrazinonicotinamide [HYNIC]-^{99m}Tc)NH_2]$ -exendin-4 conducted in Rip1Tag2 mouse model of pancreatic beta cell

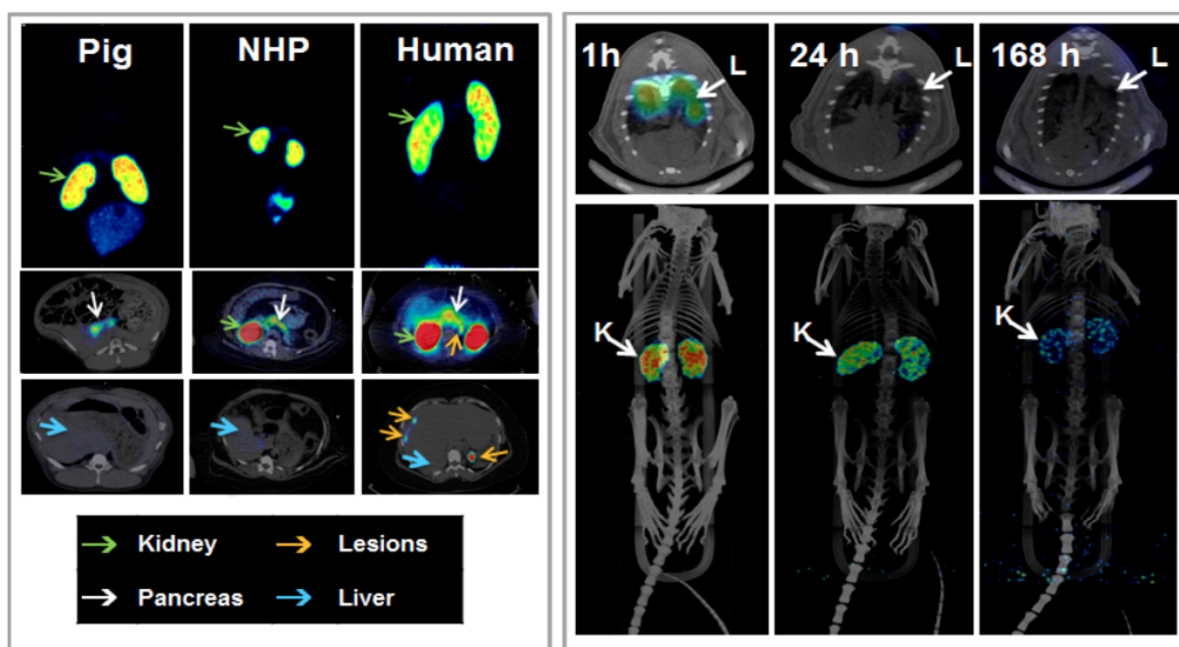


**Figure 7.** Left panel: *In vivo* biodistribution of [ $^{68}\text{Ga}$ ]Ga-DO3A-VS-Cys $^{40}$ -exendin-4 as analyzed by PET-CT imaging in the pig (0.025  $\mu\text{g}/\text{kg}$ ; 60 mi), non-human primate (NHP) (0.01  $\mu\text{g}/\text{kg}$ ; 90 min), and human (0.17  $\mu\text{g}/\text{kg}$ ; 40 min, 100 min and 120 min). The pancreas (white arrow) was delineated within 10 minutes post injection in all species. The low hepatic uptake (blue arrow) shows the potential for outlining insulinoma tumor metastasis (orange arrow, human images). The MIP coronal images demonstrate the highest uptake of the tracer in the kidneys (green arrow) in all species. Right panel: Representative fused SPECT-CT images of [ $^{177}\text{Lu}$ ]Lu-DO3A-VS-Cys $^{40}$ -exendin-4 in rats at different time points. Lungs could be outlined at 1 h p.i. and showed faster clearance in later time points (upper panel). MIP images of whole-body scan showing dominance of kidneys as excretory organ of tracer (lower panel). Reproduced from [115].

carcinogenesis showed the highest effective radiation dose from  $^{111}\text{In}$ -labeled analogue (155  $\mu\text{Sv}/\text{MBq}$ ) followed by  $^{68}\text{Ga}$ - (31.7  $\mu\text{Sv}/\text{MBq}$ ) and  $^{99\text{m}}\text{Tc}$ -labeled (3.7  $\mu\text{Sv}/\text{MBq}$ ) counterparts [69]. Comparison of various exendin-4 based imaging analogues reveals the lowest kidney dose and effective dose for  $^{68}\text{Ga}$  [95] followed by  $^{18}\text{F}$  [108],  $^{99\text{m}}\text{Tc}$  [69],  $^{64}\text{Cu}$  [78], and  $^{111}\text{In}$  [69].

[ $^{68}\text{Ga}$ ]Ga-DO3A-exendin-4/PET-CT demonstrated clinical value for the diagnostic imaging and guided surgery of insulinoma patients [26]. The subsequent receptor targeted internal radiotherapy using  $^{111}\text{Lu}$ -labeled analogue would be of considerable benefit for the treatment, however a thorough investigation of dosimetry for both [ $^{68}\text{Ga}$ ]Ga-DO3A-exendin-4 and [ $^{177}\text{Lu}$ ]Lu-DO3A-exendin-4 in rat, pig, non-human-primate and a human showed high kidney absorbed dose (Figure 7) [26, 58, 59, 94, 95].

The human extrapolated dosimetry for [ $^{68}\text{Ga}$ ]Ga-DO3A-VS-Cys $^{40}$ -exendin-4, predicted from rat, pig or NHP was favorable and potentially would allow for repeated imaging in individuals before reaching the limiting absorbed dose either in the critical organ (kidney) or the effective whole-body dose [95]. Several examinations annually would be possible allowing longitudinal studies using [ $^{68}\text{Ga}$ ]Ga-DO3A-exendin-4 and treatment response monitoring. The human predicted dosimetry for

[ $^{177}\text{Lu}$ ]Lu-DO3A-VS-Cys $^{40}$ -exendin-4 assessed from rat biodistribution also identified the kidney as the critical organ [59]. It was estimated that only approximately 4 GBq of [ $^{177}\text{Lu}$ ]Lu-DO3A-VS-Cys $^{40}$ -exendin-4 could be administered before reaching the maximal tolerated kidney dose (23 Gy) meaning that a therapeutically meaningful dose of [ $^{177}\text{Lu}$ ]Lu-DO3A-exendin-4 could cause irreversible damage to kidneys. Thus, the use of renal protective agents, or other means of reduced kidney uptake is likely required before considering [ $^{177}\text{Lu}$ ]Lu-DO3A-VS-Cys $^{40}$ -exendin-4 for insulinoma radiotherapy. Interestingly, despite the specific accumulation in the pancreatic cells, no acute diabetogenic effects in rats could be observed during a week [59].

The improvement of *in vivo* stability of exendin-based radiopharmaceuticals, as mentioned above, not only would possibly decrease the kidney uptake, but also improve the lesion uptake delivering higher radiation dose. The neutral endopeptidase (NEP) presumably causes 50% degradation of the GLP-1 ligand in blood circulation, and the inhibition of NEP improves the ligand stability [145]. The higher stability might result in the redirection of the radiopharmaceutical to the GLP-1R expressing lesions.

## Conclusions

There are unmet medical needs in both diabetes

and oncology that might be met by molecular imaging and therapy providing target specific individualized approach. Considerable progress both in radiopharmaceutical and technological development has been made during last two decades. Radiopharmaceuticals based on most commonly used metal and halogen radionuclides were developed offering various advantages. Imaging diagnostics using exendin based analogues targeted at GLP-1R in combination with SPECT and PET has proven its clinical value in insulinoma management, while many potential clinical uses in metabolic diseases including diabetes and islets transplantation are under investigation. Internal targeted radiotherapeutic application in oncology is remaining unrealized due to the unfavorable distribution and high radiation absorbed dose to kidneys. The research to reduce kidney and enhance tumor uptake continues and shows novel approaches and progress.

## Competing Interests

The authors have declared that no competing interest exists.

## References

- Ito T, Igarashi H and Jensen RT. Pancreatic neuroendocrine tumors: clinical features, diagnosis and medical treatment: advances. *Best Pract Res Clin Gastroenterol.* 2012; 26: 737-753.
- Saudek F, Brogren CH and Manohar S. Imaging the Beta-cell mass: why and how. *Rev Diabet Stud.* 2008; 5: 6-12.
- Danaei G, Finucane MM, Lu Y, Singh GM, Cowan MJ, Paciorek CJ, Lin JK, Farzadfar F, Khang YH, Stevens GA, Rao M, Ali MK, Riley LM, Robinson CA and Ezzati M. National, regional, and global trends in fasting plasma glucose and diabetes prevalence since 1980: systematic analysis of health examination surveys and epidemiological studies with 370 country-years and 2.7 million participants. *Lancet.* 2011; 378: 31-40.
- WHO Global report on diabetes. ISBN: 9789241565257. 2018; [http://apps.who.int/iris/bitstream/10665/204871/204871/9789241565257\\_eng.pdf?ua=9789241565251&ua=9789241565251](http://apps.who.int/iris/bitstream/10665/204871/204871/9789241565257_eng.pdf?ua=9789241565251&ua=9789241565251).
- International Diabetes Atlas. Diabetes Federation; IDF Diabetes Atlas; Brussels, Belgium. 2015; <http://www.diabetesatlas.org/>.
- Cnop M, Welsh N, Jonas JC, Jorns A, Lenzen S and Eizirik DL. Mechanisms of pancreatic beta-cell death in type 1 and type 2 diabetes: many differences, few similarities. *Diabetes.* 2005; 54 Suppl 2: S97-107.
- Weir GC, Bonner-Weir S and Leahy JL. Islet mass and function in diabetes and transplantation. *Diabetes.* 1990; 39: 401-405.
- Shapiro AM, Ricordi C, Hering BJ, Auchincloss H, Lindblad R, Robertson RP, Secchi A, Brendel MD, Berney T, Brennan DC, Cagliero E, Alejandro R, Ryan EA, DiMercurio B, Morel P, Polonsky KS, Reems JA, Bretzel RG, Bertuzzi F, Froud T, Kandaswamy R, Sutherland DE, Eisenbarth G, Segal M, Preiksaitis J, Korbutt GS, Barton FB, Viviano L, Seyfert-Margolis V, Bluestone J and Lakey JR. International trial of the Edmonton protocol for islet transplantation. *N Engl J Med.* 2006; 355: 1318-1330.
- Espes D, Selvaraju R, Velikyan I, Krajcovic M, Carlsson PO and Eriksson O. Quantification of beta-Cell Mass in Intramuscular Islet Grafts Using Radiolabeled Exendin-4. *Transplant Direct.* 2016; 2: e93.
- Pattou F, Kerr-Conte J and Wild D. GLP-1-Receptor Scanning for Imaging of Human Beta Cells Transplanted in Muscle. *N Engl J Med.* 2010; 363: 1289-1290.
- Moonschi FH, Hughes CB, Mussman GM, Fowlkes JL, Richards CI and Popescu I. Advances in micro- and nanotechnologies for the GLP-1-based therapy and imaging of pancreatic beta-cells. *Acta Diabetol.* 2018; 55: 405-418.
- Lappin G, Kuhnz W, Jochemsen R, Kneer J, Chaudhary A, Oosterhuis B, Drijfhout WJ, Rowland M and Garner RC. Use of microdosing to predict pharmacokinetics at the therapeutic dose: Experience with 5 drugs. *Clin Pharmacol Ther.* 2006; 80: 203-215.
- Garner RC and Lappin G. The phase 0 microdosing concept. *Br J Clin Pharmacol.* 2006; 61: 367-370.
- Bergstrom M, Grahnen A and Langstrom B. Positron emission tomography microdosing: a new concept with application in tracer and early clinical drug development. *Eur J Clin Pharmacol.* 2003; 59: 357-366.
- Manandhar B and Ahn JM. Glucagon-like peptide-1 (GLP-1) analogs: recent advances, new possibilities, and therapeutic implications. *J Med Chem.* 2015; 58: 1020-1037.
- Pan CQ, Buxton JM, Yung SL, Tom I, Yang L, Chen H, MacDougall M, Bell A, Claus TH, Clairmont KB and Whelan JP. Design of a long acting peptide functioning as both a glucagon-like peptide-1 receptor agonist and a glucagon receptor antagonist. *J Biol Chem.* 2006; 281: 12506-12515.
- Evers A, Haack T, Lorenz M, Bossart M, Elvert R, Henkel B, Stengelin S, Kurz M, Gliem M, Dudda A, Lorenz K, Kadereit D and Wagner M. Design of Novel Exendin-Based Dual Glucagon-like Peptide 1 (GLP-1)/Glucagon Receptor Agonists. *J Med Chem.* 2017; 60: 4293-4303.
- Sanchez-Garrido MA, Brandt SJ, Clemmensen C, Muller TD, DiMarchi RD and Tschop MH. GLP-1/glucagon receptor co-agonism for treatment of obesity. *Diabetologia.* 2017; 60: 1851-1861.
- Velikyan I, Haack T, Bossart M, Evers A, Laitinen I, Larsen P, Plettenburg O, Johansson L, Pierrou S, Wagner M and Eriksson O. First-in-class positron emission tomography tracer for the glucagon receptor. *EJNMMI Res.* 2019; 9: 17.
- Soga J and Yakuwa Y. Pancreatic endocrinomas: A statistical analysis of 1,857 cases. *J Hepatobiliary Pancreat Surg.* 1994; 1: 522-529.
- Öberg K and Eriksson B. Endocrine tumours of the pancreas. *Best Pract Res Clin Gastroenterol.* 19: 753-781.
- Aisha S, Lubna MZ and Huque N. Recurrent insulinoma - rare among the rarities. *J Coll Physicians Surg Pak.* 2007; 17: 364-366.
- De Herder WW, Niederle B, Scoazec JY, Pauwels S, Klöppel G, Falconi M, Kwekkeboom DJ, Öberg K, Eriksson B, Wiedenmann B, Rindi G, O'Toole D, Ferone D, Ahlman H, Arnold R, Bechstein WO, Cadiot G, Caplin M, Christ E, Chung D, Couvelard A, Delle Fave G, Falchetti A, Goretzki P, Gross D, Hochhauser D, Hyrdel R, Jensen R, Katsas G, Keleştimur F, Kianmanesh R, Knapp W, Knigge UP, Komminoth P, Körner M, Kos-Kudla B, Kvols L, Lewington V, Lopes JM, Manfredi R, McNicol AM, Mitry E, Nikou G, Nilsson O, O'Connor J, Pape UF, Pavel M, Perren A, Plöckinger U, Ramage J, Ricke J, Ruszniewski P, Salazar R, Sauvanet A, Scarpa A, Sevilla Garcia MI, Steinmüller T, Sundin A, Taal B, Van Cutsem E, Vullierme MP, Wildi S, Yao JC and Zgliczyński S. Well-differentiated pancreatic tumor/carcinoma: Insulinoma. *Neuroendocrinology.* 2006; 84: 183-188.
- Plockinger U, Rindi G, Arnold R, Eriksson B, Krenning EP, de Herder WW, Goede A, Caplin M, Öberg K, Reubi JC, Nilsson O, Delle Fave G, Ruszniewski P, Ahlman H, Wiedenmann B and European Neuroendocrine Tumour Society. Guidelines for the diagnosis and treatment of neuroendocrine gastrointestinal tumours. A consensus statement on behalf of the European Neuroendocrine Tumour Society (ENETS). *Neuroendocrinology.* 2004; 80: 394-424.
- Chatziioannou A, Kehagias D, Mourikis D, Antoniou A, Limouris G, Kaponis A, Kavatzas N, Tseleni S and Vlachos L. Imaging and localization of pancreatic insulinomas. *Clin Imaging.* 2001; 25: 275-283.
- Eriksson O, Velikyan I, Selvaraju RK, Kandeel F, Johansson L, Antoni G, Eriksson B, Sörensen J and Korsgren O. Detection of metastatic insulinoma by positron emission tomography with [<sup>68</sup>Ga]exendin-4-A case report. *J Clin Endocrinol Metab.* 2014; 99: 1519-1524.
- McAuley G, Delaney H, Colville J, Lyburn I, Worsley D, Govender P and Torreggiani WC. Multimodality preoperative imaging of pancreatic insulinomas. *Clin Radiol.* 2005; 60: 1039-1050.
- Okabayashi T, Shima Y, Sumiyoshi T, Kozuki A, Ito S, Ogawa Y, Kobayashi M and Hanazaki K. Diagnosis and management of insulinoma. *World J Gastroenterol.* 2013; 19: 829-837.
- Krenning EP, Kwekkeboom DJ, Reubi JC, Van Hagen PM, van Eijck CHJ, Oei HY and Lamberts SWJ. <sup>111</sup>In-octreotide scintigraphy in oncology. *Metabolism.* 1992; 41: 83-86.
- Krenning EP, Kwekkeboom DJ, Bakker WH, Breeman WA, Kooij PP, Oei HY, van Hagen M, Postema PT, de Jong M, Reubi JC and et al. Somatostatin receptor scintigraphy with [<sup>111</sup>In-DTPA-D-Phe<sup>1</sup>] and [<sup>123</sup>I-Tyr<sup>3</sup>]octreotide: the Rotterdam experience with more than 1000 patients. *Eur J Nucl Med.* 1993; 20: 716-731.
- Reubi JC. Peptide receptors as molecular targets for cancer diagnosis and therapy. *Endocr Rev.* 2003; 24: 389-427.
- Korner M, Stockli M, Waser B and Reubi JC. GLP-1 receptor expression in human tumors and human normal tissues: potential for in vivo targeting. *J Nucl Med.* 2007; 48: 736-743.
- Reubi JC and Waser B. Concomitant expression of several peptide receptors in neuroendocrine tumours: molecular basis for in vivo multireceptor tumour targeting. *Eur J Nucl Med Mol Imaging.* 2003; V30: 781-793.
- Fidler JL. Preoperative Detection of Pancreatic Insulinomas on Multiphasic Helical CT. *Am J of Roentgenol.* 1976; 181: 775-780.
- Sotoudehmanesh R. Hedayat A, Shirazian N, Shahraeeni S, Ainechi S, Zeinali F, Kolahdoozan S. Endoscopic ultrasonography (EUS) in the localization of insulinoma. *Endocrine.* 2007; 31: 238-241.
- Rostambeigi N. What should be done in an operating room when an insulinoma cannot be found? *Clin endocrinol.* 2009; 70: 512-515.
- Wild D, Christ E, Caplin ME, Kurzwinski TR, Forrer F, Brandle M, Seufert J, Weber WA, Bomanji J, Perren A, Ell PJ and Reubi JC. Glucagon-like peptide-1 versus somatostatin receptor targeting reveals 2 distinct forms of malignant insulinomas. *J Nucl Med.* 2011; 52: 1073-1078.
- Luo Y, Pan Q, Yao S, Yu M, Wu W, Xue H, Kiesewetter DO, Zhu Z, Li F, Zhao Y and Chen X. Glucagon-Like Peptide-1 Receptor PET/CT with

- 68Ga-NOTA-Exendin-4 for Detecting Localized Insulinoma: A Prospective Cohort Study. *J Nucl Med*. 2016; 57: 715-720.
39. Sowa-Staszczak A, Trofimiuk-Muldner M, Stefanska A, Tomaszuk M, Buziak-Bereza M, Gilis-Januszewska A, Jabrocka-Hybel A, Glowa B, Malecki M, Bednarczuk T, Kaminski G, Kowalska A, Mikolajczak R, Janota B and Hubalewska-Dydejczyk A. <sup>99m</sup>Tc Labeled Glucagon-Like Peptide-1-Analogue (<sup>99m</sup>Tc-GLP1) Scintigraphy in the Management of Patients with Occult Insulinoma. *PLoS One*. 2016; 11: e0160714.
  40. Bongetti E, Lee MH, Pattison DA, Hicks RJ, Norris R, Sachithanandan N and MacIsaac RJ. Diagnostic challenges in a patient with an occult insulinoma: (68)Ga-DOTA-exendin-4 PET/CT and (68)Ga-DOTATATE PET/CT. *Clin Case Rep*. 2018; 6: 719-722.
  41. Körner M, Christ E, Wild D and Reubi JC. Glucagon-like peptide-1 receptor overexpression in cancer and its impact on clinical applications. *Front Endocrinol (Lausanne)*. 2012; 3:158.
  42. Richards P, Parker HE, Adriaenssens AE, Hodgson JM, Cork SC, Trapp S, Gribble FM and Reimann F. Identification and characterization of GLP-1 receptor-expressing cells using a new transgenic mouse model. *Diabetes*. 2014; 63: 1224-1233.
  43. Tornehave D, Kristensen P, Romer J, Knudsen LB and Heller RS. Expression of the GLP-1 receptor in mouse, rat, and human pancreas. *J Histochem Cytochem*. 2008; 56: 841-851.
  44. Wang X, Misawa R, Zielinski MC, Cowen P, Jo J, Periwal V, Ricordi C, Khan A, Szust J, Shen J, Millis JM, Witkowski P and Hara M. Regional differences in islet distribution in the human pancreas--preferential beta-cell loss in the head region in patients with type 2 diabetes. *PLoS One*. 2013; 8: e67454.
  45. Kirk RK, Pyke C, von Herrath MG, Hasselby JP, Pedersen L, Mortensen PG, Knudsen LB and Coppieters K. Immunohistochemical assessment of glucagon-like peptide 1 receptor (GLP-1R) expression in the pancreas of patients with type 2 diabetes. *Diabetes Obes Metab*. 2017; 19: 705-712.
  46. Eriksson O, Rosenstrom U, Selvaraju RK, Eriksson B and Velikyan I. Species differences in pancreatic binding of DO3A-VS-Cys(40)-Exendin4. *Acta Diabetol*. 2017; 54: 1039-1045.
  47. Brubaker PL and Drucker DJ. Minireview: Glucagon-like peptides regulate cell proliferation and apoptosis in the pancreas, gut, and central nervous system. *Endocrinology*. 2004; 145: 2653-2659.
  48. Deacon CF, Nauck MA, Toft-Nielsen M, Pridal L, Willms B and Holst JJ. Both subcutaneously and intravenously administered glucagon-like peptide I are rapidly degraded from the NH2-terminus in type II diabetic patients and in healthy subjects. *Diabetes*. 1995; 44: 1126-1131.
  49. Finan B, Clemmensen C and Muller TD. Emerging opportunities for the treatment of metabolic diseases: Glucagon-like peptide-1 based multi-agonists. *Mol Cell Endocrinol*. 2015; 418 Pt 1: 42-54.
  50. Eng J, Kleinman WA, Singh L, Singh G and Raufman JP. Isolation and characterization of exendin-4, an exendin-3 analogue, from *Heloderma suspectum* venom. Further evidence for an exendin receptor on dispersed acini from guinea pig pancreas. *J Biol Chem*. 1992; 267: 7402-7405.
  51. Runge S, Schimmer S, Oschmann J, Schiodt CB, Knudsen SM, Jeppesen CB, Madsen K, Lau J, Thogersen H and Rudolph R. Differential structural properties of GLP-1 and exendin-4 determine their relative affinity for the GLP-1 receptor N-terminal extracellular domain. *Biochemistry*. 2007; 46: 5830-5840.
  52. Runge S, Thogersen H, Madsen K, Lau J and Rudolph R. Crystal structure of the ligand-bound glucagon-like peptide-1 receptor extracellular domain. *J Biol Chem*. 2008; 283: 11340-11347.
  53. Gotthardt M, Fischer M, Naehrer I, Holz JB, Junglas H, Fritsch HW, Behe M, Goke B, Joseph K and Behr TM. Use of the incretin hormone glucagon-like peptide-1 (GLP-1) for the detection of insulinomas: initial experimental results. *Eur J Nucl Med Mol Imaging*. 2002; 29: 597-606.
  54. Eriksson O, Laughlin M, Brom M, Nuutila P, Roden M, Hwa A, Bonadonna R and Gotthardt M. In vivo imaging of beta cells with radiotracers: state of the art, prospects and recommendations for development and use. *Diabetologia*. 2016; 59: 1340-1349.
  55. Rahier J, Guiot Y, Goebbels RM, Sempoux C and Henquin JC. Pancreatic beta-cell mass in European subjects with type 2 diabetes. *Diabetes Obes Metab*. 2008; 4: 32-42.
  56. Sweet IR, Cook DL, Lernmark A, Greenbaum CJ and Krohn KA. Non-invasive imaging of beta cell mass: a quantitative analysis. *Diabetes Technol Ther*. 2004; 6: 652-659.
  57. Brom M, Woliner-van der Weg W, Joosten L, Frielink C, Bouckenoooghe T, Rijken P, Andralojc K, Goke BJ, de Jong M, Eizirik DL, Behe M, Lahoutte T, Oyen WJ, Tack CJ, Janssen M, Boerman OC and Gotthardt M. Non-invasive quantification of the beta cell mass by SPECT with (1)(1)In-labelled exendin. *Diabetologia*. 2014; 57: 950-959.
  58. Selvaraju RK, Velikyan I, Johansson L, Wu Z, Todorov I, Shively J, Kandeel F, Korsgren O and Eriksson O. In vivo imaging of the glucagonlike peptide 1 receptor in the pancreas with 68Ga-labeled DO3A-exendin-4. *J Nucl Med*. 2013; 54: 1458-1463.
  59. Velikyan I, Bulenga TN, Selvaraju KR, Lubberink M, Espes D, Rosenstrom U and Eriksson O. Dosimetry of [<sup>177</sup>Lu]-DO3A-VS-Cys40-Exendin-4 - impact on the feasibility of insulinoma internal radiotherapy. *Am J Nucl Med Mol Imaging*. 2015; 5: 109-126.
  60. Brom M, Joosten L, Frielink C, Boerman O and Gotthardt M. (111)In-exendin uptake in the pancreas correlates with the beta-cell mass and not with the alpha-cell mass. *Diabetes*. 2015; 64: 1324-1328.
  61. Deacon CF. Circulation and degradation of GIP and GLP-1. *Horm Metab Res*. 2004; 36: 761-765.
  62. Gotthardt M, Lalyko G, van Eerd-Vismale J, Keil B, Schurrat T, Hower M, Laverman P, Behr TM, Boerman OC, Göke B and Béhé M. A new technique for in vivo imaging of specific GLP-1 binding sites: First results in small rodents. *Regul Pept*. 2006; 137: 162-167.
  63. Wild D, Behe M, Wicki A, Storch D, Waser B, Gotthardt M, Keil B, Christofori G, Reubi JC and Macke HR. [Lys40(Ahx-DTPA-111In)NH2]exendin-4, a very promising ligand for glucagon-like peptide-1 (GLP-1) receptor targeting. *J Nucl Med*. 2006; 47: 2025-2033.
  64. Wild D, Macke H, Christ E, Gloor B and Reubi JC. Glucagon-like peptide 1-receptor scans to localize occult insulinomas. *N Engl J Med*. 2008; 359: 766-768.
  65. Sowa-Staszczak A, Pach D, Mikolajczak R, Macke H, Jabrocka-Hybel A, Stefanska A, Tomaszuk M, Janota B, Gilis-Januszewska A, Malecki M, Kaminski G, Kowalska A, Kulig J, Matyja A, Osuch C and Hubalewska-Dydejczyk A. Glucagon-like peptide-1 receptor imaging with [Lys40(Ahx-HYNIC- <sup>99m</sup>Tc/EDDA)NH2]-exendin-4 for the detection of insulinoma. *Eur J Nucl Med Mol Imaging*. 2013; 40: 524-531.
  66. Christ E, Wild D, Forrer F, Brandl M, Sahli R, Clerici T, Gloor B, Martius F, Maecke H and Reubi JC. Glucagon-like peptide-1 receptor imaging for localization of insulinomas. *J Clin Endocrinol Metab*. 2009; 94: 4398-4405.
  67. Brom M, Joosten L, Oyen WJG, Gotthardt M and Boerman OC. Radiolabelled GLP-1 analogues for in vivo targeting of insulinomas. *Contrast Media Mol Imaging*. 2012; 7: 160-166.
  68. Brom M, Oyen WJ, Joosten L, Gotthardt M and Boerman OC. 68Ga-labelled exendin-3, a new agent for the detection of insulinomas with PET. *Eur J Nucl Med Mol Imaging*. 2010; 37: 1345-1355.
  69. Wild D, Wicki A, Mansi R, Behe M, Keil B, Bernhardt P, Christofori G, Ell PJ and Macke HR. Exendin-4-Based Radiopharmaceuticals for Glucagonlike Peptide-1 Receptor PET/CT and SPECT/CT. *J Nucl Med*. 2010; 51: 1059-1067.
  70. Selvaraju RK, Velikyan I, Asplund V, Johansson L, Wu Z, Todorov I, Shively J, Kandeel F, Eriksson B, Korsgren O and Eriksson O. Pre-clinical evaluation of [68Ga]Ga-DO3A-VS-Cys40-Exendin-4 for imaging of insulinoma. *Nucl Med Biol*. 2014; 41: 471-476.
  71. Wu Z, Liu S, Nair I, Omori K, Scott S, Todorov I, Shively JE, Conti PS, Li Z and Kandeel F. (64)Cu labeled sarcophagine exendin-4 for microPET imaging of glucagon like peptide-1 receptor expression. *Theranostics*. 2014; 4: 770-777.
  72. Wang Y, Lim K, Normandin M, Zhao X, Cline GW and Ding YS. Synthesis and evaluation of [18F]exendin (9-39) as a potential biomarker to measure pancreatic beta-cell mass. *Nucl Med Biol*. 2012; 39: 167-176.
  73. Gao H, Niu G, Yang M, Quan Q, Ma Y, Murage EN, Ahn JM, Kiesewetter DO and Chen X. PET of insulinoma using (1)(8)F-FBEM-EM3106B, a new GLP-1 analogue. *Mol Pharm*. 2011; 8: 1775-1782.
  74. Kiesewetter DO, Gao H, Ma Y, Niu G, Quan Q, Guo N and Chen X. 18F-radiolabeled analogs of exendin-4 for PET imaging of GLP-1 in insulinoma. *Eur J Nucl Med Mol Imaging*. 2012; 39: 463-473.
  75. Luo Y, Yu M, Pan Q, Wu W, Zhang T, Kiesewetter DO, Zhu Z, Li F, Chen X and Zhao Y. 68Ga-NOTA-exendin-4 PET/CT in detection of occult insulinoma and evaluation of physiological uptake. *Eur J Nucl Med Mol Imaging*. 2015; 42: 531-532.
  76. Christ E, Wild D, Antwi K, Waser B, Fani M, Schwanda S, Heye T, Schmid C, Baer HU, Perren A and Reubi JC. Preoperative localization of adult nesidioblastosis using 68Ga-DOTA-exendin-4-PET/CT. *Endocrine*. 2015; 50: 821-823.
  77. Jodal A, Lankat-Buttgereit B, Brom M, Schibli R and Behe M. A comparison of three (67/68)Ga-labelled exendin-4 derivatives for beta-cell imaging on the GLP-1 receptor: the influence of the conjugation site of NODAGA as chelator. *EJNMMI Res*. 2014; 4: 31.
  78. Kirsi M, Yim CB, Veronica F, Tamiko I, Viki-Veikko E, Johan R, Jori J, Tiina S, Tuula T, Marko T, Eleni G, Martin B, Martin G, Claude RJ, Helmut M, Anne R, Olof S and Pirjo N. 64Cu- and 68Ga-Labelled [Nle14,Lys 40(Ahx-NODAGA)NH2]-Exendin-4 for pancreatic beta cell imaging in rats. *Mol Imaging Biol*. 2014; 16: 255-263.
  79. Wu Z, Todorov I, Li L, Bading JR, Li Z, Nair I, Ishiyama K, Colcher D, Conti PE, Fraser SE, Shively JE and Kandeel F. In vivo imaging of transplanted islets with 64Cu-DO3A-VS-Cys40-Exendin-4 by targeting GLP-1 receptor. *Bioconjug Chem*. 2011; 22: 1587-1594.
  80. Kiesewetter DO, Guo N, Guo J, Gao H, Zhu L, Ma Y, Niu G and Chen X. Evaluation of an [(18)F]AlF-NOTA Analog of Exendin-4 for Imaging of GLP-1 Receptor in Insulinoma. *Theranostics*. 2012; 2: 999-1009.
  81. Yue X, Kiesewetter DO, Guo J, Sun Z, Zhang X, Zhu L, Niu G, Ma Y, Lang L and Chen X. Development of a New Thiol Site-Specific Prosthetic Group and Its Conjugation with [Cys40]-exendin-4 for in Vivo Targeting of Insulinomas. *Bioconjug Chem*. 2013; 24: 1191-1200.
  82. Yue X, Yan X, Wu C, Niu G, Ma Y, Jacobson O, Shen B, Kiesewetter DO and Chen X. One-pot two-step radiosynthesis of a new (18)F-labeled thiol reactive prosthetic group and its conjugate for insulinoma imaging. *Mol Pharm*. 2014; 11: 3875-3884.
  83. Wu H, Liang S, Liu S, Pan Y, Cheng D and Zhang Y. 18F-radiolabeled GLP-1 analog exendin-4 for PET/CT imaging of insulinoma in small animals. *Nucl Med Commun*. 2013; 34: 701-708.
  84. Wu Z, Liu S, Hassink M, Nair I, Park R, Li L, Todorov I, Fox JM, Li Z, Shively JE, Conti PS and Kandeel F. Development and evaluation of

- 18F-TTCO-Cys40-Exendin-4: a PET probe for imaging transplanted islets. *J Nucl Med.* 2013; 54: 244-251.
85. Bauman A, Valverde IE, Fischer CA, Vomstein S and Mindt TL. Development of 68Ga- and 89Zr-Labeled Exendin-4 as Potential Radiotracers for the Imaging of Insulinomas by PET. *J Nucl Med.* 2015; 56: 1569-1574.
86. Janota B, Karczmarczyk U, Laszuk E, Garnuszek P and Mikolajczak R. Oxidation of methionine - is it limiting the diagnostic properties of 99mTc-labeled Exendin-4, a Glucagon-Like Peptide-1 receptor agonist? *Nucl Med Rev Cent East Eur.* 2016; 19: 104-110.
87. Antwi K, Fani M, Nicolas G, Rottenburger C, Heye T, Reubi JC, Gloor B, Christ E and Wild D. Localization of Hidden Insulinomas with 68Ga-DOTA-Exendin-4 PET/CT: A Pilot Study. *J Nucl Med.* 2015; 56: 1075-1078.
88. Wicki A, Wild D, Storch D, Seemayer C, Gotthardt M, Behe M, Kneifel S, Mihatsch MJ, Reubi JC, Macke HR and Christofori G. [Lys40(Ahx-DTPA-111In)NH2]-Exendin-4 is a highly efficient radiotherapeutic for glucagon-like peptide-1 receptor-targeted therapy for insulinoma. *Clin Cancer Res.* 2007; 13: 3696-3705.
89. Kimura H, Fujita N, Kanbe K, Matsuda H, Watanabe H, Arimitsu K, Fujimoto H, Hamamatsu K, Yagi Y, Ono M, Inagaki N and Saji H. Synthesis and biological evaluation of an (111)In-labeled exendin-4 derivative as a single-photon emission computed tomography probe for imaging pancreatic beta-cells. *Bioorg Med Chem.* 2017; 25: 5772-5778.
90. Kimura H, Matsuda H, Ogawa Y, Fujimoto H, Toyoda K, Fujita N, Arimitsu K, Hamamatsu K, Yagi Y, Ono M, Inagaki N and Saji H. Development of (111)In-labeled exendin(9-39) derivatives for single-photon emission computed tomography imaging of insulinoma. *Bioorg Med Chem.* 2017; 25: 1406-1412.
91. Seo D, Faintuch BL, Aparecida de Oliveira E and Faintuch J. Pancreas and liver uptake of new radiolabeled incretins (GLP-1 and Exendin-4) in models of diet-induced and diet-restricted obesity. *Nucl Med Biol.* 2017; 49: 57-64.
92. Medina-Garcia V, Ocampo-Garcia BE, Ferro-Flores G, Santos-Cuevas CL, Aranda-Lara L, Garcia-Becerra R, Ordaz-Rosado D and Melendez-Alafort L. A freeze-dried kit formulation for the preparation of Lys(27)(99mTc-EDDA/HYNIC)-Exendin(9-39)/99mTc-EDDA/HYNIC-Tyr3-Octreotide to detect benign and malignant insulinomas. *Nucl Med Biol.* 2015; 42: 911-916.
93. Velikyan I, Rosenstrom U and Eriksson O. Fully automated GMP production of [68Ga]Ga-DO3A-VS-Cys40-Exendin-4 for clinical use. *Am J Nucl Med Mol Imaging.* 2017; 7: 111-125.
94. Nalin L, Selvaraju RK, Velikyan I, Berglund M, Andreasson S, Wikstrand A, Ryden A, Lubberink M, Kandeel F, Nyman G, Korsgren O, Eriksson O and Jensen-Waern M. Positron emission tomography imaging of the glucagon-like peptide-1 receptor in healthy and streptozotocin-induced diabetic pigs. *Eur J Nucl Med Mol Imaging.* 2014; 41: 1800-1810.
95. Selvaraju R, Bulenga TN, Espes D, Lubberink M, Sörensen J, Eriksson B, Estrada S, Velikyan I and Eriksson O. Dosimetry of [68Ga]Ga-DO3A-VS-Cys40-Exendin-4 in rodents, pigs, non-human primates and human - repeated scanning in human is possible. *Am J Nucl Med Mol Imaging.* 2015; 5: 259-269.
96. Ryden A, Nyman G, Nalin L, Andreasson S, Velikyan I, Korsgren O, Eriksson O and Jensen-Waern M. Corrigendum to "Cardiovascular side-effects and insulin secretion after intravenous administration of radiolabeled Exendin-4 in pigs" [*Nucl Med Biol* 43 (2016) 397-402]. *Nucl Med Biol.* 2016; 43: 742.
97. Ryden A, Nyman G, Nalin L, Andreasson S, Velikyan I, Korsgren O, Eriksson O and Jensen-Waern M. Cardiovascular side-effects and insulin secretion after intravenous administration of radiolabeled Exendin-4 in pigs. *Nucl Med Biol.* 2016; 43: 397-402.
98. Zhang M, Jacobson O, Kiesewetter DO, Ma Y, Wang Z, Lang L, Tang L, Kang F, Deng H, Yang W, Niu G, Wang J and Chen X. Improving the Theranostic Potential of Exendin 4 by Reducing the Renal Radioactivity through Brush Border Membrane Enzyme-Mediated Degradation. *Bioconjug Chem.* 2019; 30: 1745-1753.
99. Yim C-B, Mikkola K, Fagerholm V, Elomaa V-V, Ishizu T, Rajander J, Schlesinger J, Roivainen A, Nuutila P and Solin O. Synthesis and preclinical characterization of [64Cu]NODAGA-MAL-exendin-4 with a Nε-maleoyl-L-lysyl-glycine linkage. *Nucl Med Biol.* 2013; 40: 1006-1012.
100. Cai Z and Anderson CJ. Chelators for copper radionuclides in positron emission tomography radiopharmaceuticals. *J Labelled Comp Radiopharm.* 2014; 57: 224-230.
101. Brand C, Abdel-Atti D, Zhang Y, Carlin S, Clardy SM, Keliher EJ, Weber WA, Lewis JS and Reiner T. In vivo imaging of GLP-1R with a targeted bimodal PET/fluorescence imaging agent. *Bioconjug Chem.* 2014; 25: 1323-1330.
102. Boerman OC and Gotthardt M. 18F-Labelled exendin to image GLP-1 receptor-expressing tissues: from niche to blockbuster? *Eur J Nucl Med Mol Imaging.* 2012; 39: 461-462.
103. Xu Y, Pan D, Xu Q, Zhu C, Wang L, Chen F, Yang R, Luo S and Yang M. Insulinoma imaging with glucagon-like peptide-1 receptor targeting probe (18F)-FBEM-Cys (39)-exendin-4. *J Cancer Res Clin Oncol.* 2014; 140: 1479-1488.
104. Dialer LO, Jodal A, Schibli R, Ametamey SM and Behe M. Radiosynthesis and evaluation of an (18F)-labeled silicon containing exendin-4 peptide as a PET probe for imaging insulinoma. *EJNMMI Radiopharm Chem.* 2018; 3: 1.
105. Kimura H, Ogawa Y, Fujimoto H, Mukai E, Kawashima H, Arimitsu K, Toyoda K, Fujita N, Yagi Y, Hamamatsu K, Murakami T, Murakami A, Ono M, Nakamoto Y, Togashi K, Inagaki N and Saji H. Evaluation of (18F)-labeled exendin(9-39) derivatives targeting glucagon-like peptide-1 receptor for pancreatic beta-cell imaging. *Bioorg Med Chem.* 2018; 26: 463-469.
106. Xu Q, Zhu C, Xu Y, Pan D, Liu P, Yang R, Wang L, Chen F, Sun X, Luo S and Yang M. Preliminary evaluation of [18F]AIF-NOTA-MAL-Cys39-exendin-4 in insulinoma with PET. *J Drug Target.* 2015; 23: 813-820.
107. Keliher EJ, Reiner T, Thurber GM, Upadhyay R and Weissleder R. Efficient (18F)-Labeling of Synthetic Exendin-4 Analogues for Imaging Beta Cells. *ChemistryOpen.* 2012; 1: 177-183.
108. Mikkola K, Yim CB, Lehtiniemi P, Kauhanen S, Tarkia M, Tolvanen T, Nuutila P and Solin O. Low kidney uptake of GLP-1R-targeting, beta cell-specific PET tracer, (18F)-labeled [Nle(14),Lys(40)]exendin-4 analog, shows promise for clinical imaging. *EJNMMI Res.* 2016; 6: 91.
109. Mukai E, Toyoda K, Kimura H, Kawashima H, Fujimoto H, Ueda M, Temma T, Hirao K, Nagakawa K, Saji H and Inagaki N. GLP-1 receptor antagonist as a potential probe for pancreatic β-cell imaging. *Biochem Biophys Res Commun.* 2009; 389: 523-526.
110. Waser B and Reubi JC. Value of the radiolabelled GLP-1 receptor antagonist exendin(9-39) for targeting of GLP-1 receptor-expressing pancreatic tissues in mice and humans. *Eur J Nucl Med Mol Imaging.* 2011; 38: 1054-1058.
111. Waser B and Reubi JC. Radiolabelled GLP-1 receptor antagonist binds to GLP-1 receptor-expressing human tissues. *Eur J Nucl Med Mol Imaging.* 2014; 41: 1166-1171.
112. Lappchen T, Tonnesmann R, Eersels J, Meyer PT, Maecke HR and Rylova SN. Radioiodinated Exendin-4 Is Superior to the Radiometal-Labelled Glucagon-Like Peptide-1 Receptor Probes Overcoming Their High Kidney Uptake. *PLoS One.* 2017; 12: e0170435.
113. Lv J, Pan Y, Li X, Cheng D, Liu S, Shi H and Zhang Y. The imaging of insulinomas using a radionuclide-labelled molecule of the GLP-1 analogue liraglutide: a new application of liraglutide. *PLoS One.* 2014; 9: e96833.
114. Kirkpatrick A, Heo J, Abrol R and Goddard WA, 3rd. Predicted structure of agonist-bound glucagon-like peptide 1 receptor, a class B G protein-coupled receptor. *Proc Natl Acad Sci U S A.* 2012; 109: 19988-19993.
115. Velikyan I. 68Ga-Based Radiopharmaceuticals: Production and Application Relationship. *Molecules.* 2015; 20: 12913-12943.
116. Sako T, Hasegawa K, Nishimura M, Kanayama Y, Wada Y, Hayashinaka E, Cui Y, Kataoka Y, Senda M and Watanabe Y. Positron emission tomography study on pancreatic somatostatin receptors in normal and diabetic rats with 68Ga-DOTA-octreotide: A potential PET tracer for beta cell mass measurement. *Biochem Biophys Res Commun.* 2013; 442: 79-84.
117. Velikyan I. Prospective of 68Ga-Radiopharmaceutical development. *Theranostics.* 2014; 4: 47-80.
118. Joosten L, Brom M, Peeters H, Heskamp S, Behe M, Boerman O and Gotthardt M. Enhanced Specific Activity by Multichelation of Exendin-3 Leads To Improved Image Quality and In Vivo Beta Cell Imaging. *Mol Pharm.* 2018; 15: 486-494.
119. Eter WA, Bos D, Frielink C, Boerman OC, Brom M and Gotthardt M. Graft revascularization is essential for non-invasive monitoring of transplanted islets with radiolabeled exendin. *Sci Rep.* 2015; 5: 15521.
120. Joosten L, Brom M, D B, Frielink C, Peeters H, Himpe E, L. Bouwens, Boerman OC and Gotthardt M. Abstracts of 51st EASD Annual Meeting. *Diabetologia.* 2015; 58: 1-607.
121. Mathijs I, Xavier C, Peleman C, Caveliers V, Brom M, Gotthardt M, Herrera PL, Lahoutte T and Bouwens L. A standardized method for in vivo mouse pancreas imaging and semiquantitative beta cell mass measurement by dual isotope SPECT. *Mol Imaging Biol.* 2015; 17: 58-66.
122. Willekens SM, Joosten L, Boerman OC, Balhuizen A, Eizirik DL, Gotthardt M and Brom M. Strain Differences Determine the Suitability of Animal Models for Noninvasive In Vivo Beta Cell Mass Determination with Radiolabeled Exendin. *Mol Imaging Biol.* 2016; 18: 705-714.
123. Khera E, Zhang L, Roberts S, Nessler I, Sandoval D, Reiner T and Thurber G. Blocking Glucagon Like Peptide-1 Receptors in the Exocrine Pancreas Improves Specificity for Beta Cells in a Mouse Model of Type 1 Diabetes. *J Nucl Med.* 2019;
124. Connolly BM, Vanko A, McQuade P, Guenther I, Meng X, Rubins D, Waterhouse R, Hargreaves R, Sur C and Hostetler E. Ex vivo imaging of pancreatic beta cells using a radiolabeled GLP-1 receptor agonist. *Mol Imaging Biol.* 2012; 14: 79-87.
125. Monazzam A, Lau J, Velikyan I, Li SC, Razmara M, Rosenstrom U, Eriksson O and Skogseid B. Increased Expression of GLP-1R in Proliferating Islets of Men1 Mice is Detectable by [(68)Ga]Ga-DO3A-VS-Cys(40)-Exendin-4 /PET. *Sci Rep.* 2018; 8: 748.
126. Gao H, Kiesewetter DO, Zhang X, Huang X, Guo N, Lang L, Hida N, Wang H, Wang H, Cao F, Niu G and Chen X. PET of glucagonlike peptide receptor upregulation after myocardial ischemia or reperfusion injury. *J Nucl Med.* 2012; 53: 1960-1968.
127. Stahle M, Kyto V, Kiugel M, Liljenback H, Metsala O, Kakela M, Li XG, Oikonen V, Saukko P, Nuutila P, Knuuti J, Roivainen A and Saraste A. Glucagon-like peptide-1 receptor expression after myocardial infarction: Imaging study using (68)Ga-NODAGA-exendin-4 positron emission tomography. *J Nucl Cardiol.* 2018;
128. Rylova SN, Waser B, Del Pozzo L, Tonnesmann R, Mansi R, Meyer PT, Reubi JC and Maecke HR. Approaches to Improve the Pharmacokinetics of Radiolabeled Glucagon-Like Peptide-1 Receptor Ligands Using Antagonistic Tracers. *J Nucl Med.* 2016; 57: 1282-1288.

129. Hamamatsu K, Fujimoto H, Fujita N, Murakami T, Kimura H, Saji H and Inagaki N. Establishment of a method for in-vivo SPECT/CT imaging analysis of <sup>111</sup>In-labeled exendin-4 pancreatic uptake in mice without the need for nephrectomy or a secondary probe. *Nucl Med Biol.* 2018; 64-65: 22-27.
130. Melis M, Vegt E, Konijnenberg MW, de Visser M, Bijster M, Vermeij M, Krenning EP, Boerman OC and de Jong M. Nephrotoxicity in mice after repeated imaging using <sup>111</sup>In-labeled peptides. *J Nucl Med.* 2010; 51: 973-977.
131. Bullock BP, Heller RS and Habener JF. Tissue distribution of messenger ribonucleic acid encoding the rat glucagon-like peptide-1 receptor. *Endocrinology.* 1996; 137: 2968-2978.
132. Duncan JR, Stephenson MT, Wu HP and Anderson CJ. Indium-111-diethylenetriaminepentaacetic acid-octreotide is delivered in vivo to pancreatic, tumor cell, renal, and hepatocyte lysosomes. *Cancer Res.* 1997; 57: 659-671.
133. Behr TM, Goldenberg DM and Becker W. Reducing the renal uptake of radiolabeled antibody fragments and peptides for diagnosis and therapy: present status, future prospects and limitations. *Eur J Nucl Med.* 1998; 25: 201-212.
134. Bodei L, Mueller-Brand J, Baum RP, Pavel ME, Horsch D, O'Dorisio MS, O'Dorisio TM, Howe JR, Cremonesi M, Kwekkeboom DJ and Zaknun JJ. The joint IAEA, EANM, and SNMMI practical guidance on peptide receptor radionuclide therapy (PRRT) in neuroendocrine tumours. *Eur J Nucl Med Mol Imaging.* 2013; 40: 800-816.
135. Vegt E, Melis M, Eek A, de Visser M, Brom M, Oyen WJG, Gotthardt M, de Jong M and Boerman OC. Renal uptake of different radiolabelled peptides is mediated by megalin: SPECT and biodistribution studies in megalin-deficient mice. *Eur J Nucl Med Mol Imaging.* 2011; 38: 623-632.
136. Vegt E, van Eerd JE, Eek A, Oyen WJ, Wetzels JF, de Jong M, Russel FG, Masereeuw R, Gotthardt M and Boerman OC. Reducing renal uptake of radiolabeled peptides using albumin fragments. *J Nucl Med.* 2008; 49: 1506-1511.
137. Gotthardt M, Van Eerd-Vismale J, Oyen WJG, De Jong M, Zhang H, Rolleman E, Maecke HR, Béhé M and Boerman O. Indication for different mechanisms of kidney uptake of radiolabeled peptides. *J Nucl Med.* 2007; 48: 596-601.
138. Buitinga M, Jansen T, van der Kroon I, Woliner-van der Weg W, Boss M, Janssen M, Aarntzen E, Béhé M, Wild D, Visser E, Brom M and Gotthardt M. Succinylated Gelatin Improves the Theranostic Potential of Radiolabeled Exendin-4 in Insulinoma Patients. *J Nucl Med.* 2019; 60: 812-816.
139. Vegt E, Eek A, Oyen WJG, de Jong M, Gotthardt M and Boerman OC. Albumin-derived peptides efficiently reduce renal uptake of radiolabeled peptides. *Eur J Nucl Med Mol Imaging.* 2010; 37: 226-234.
140. Laeppchen T, Toennesmann R, Meyer P, Maecke H and Rylova S. Radioiodinated exendin-4 demonstrates superior pharmacokinetics compared to radiometalated analogs. *J Nucl Med.* 2016; 57: 1388.
141. Eriksson O, Korsgren O, Selvaraju RK, Mollaret M, de Boysson Y, Chimienti F and Altai M. Pancreatic imaging using an antibody fragment targeting the zinc transporter type 8: a direct comparison with radio-iodinated Exendin-4. *Acta Diabetol.* 2018; 55: 49-57.
142. Zechmann CM, Afshar-Oromieh A, Armor T, Stubbs JB, Mier W, Hadaschik B, Joyal J, Kopka K, Debus J, Babich JW and Haberkorn U. Radiation dosimetry and first therapy results with a (<sup>124</sup>I)/ (<sup>131</sup>I)-labeled small molecule (MIP-1095) targeting PSMA for prostate cancer therapy. *Eur J Nucl Med Mol Imaging.* 2014; 41: 1280-1292.
143. Mier W, Kratochwil C, Hassel JC, Giesel FL, Beijer B, Babich JW, Friebe M, Eisenhut M, Enk A and Haberkorn U. Radiopharmaceutical Therapy of Patients with Metastasized Melanoma with the Melanin-Binding Benzamide <sup>131</sup>I-BA52. *J Nucl Med.* 2014; 55: 9-14.
144. Simonsen L, Holst JJ and Deacon CF. Exendin-4, but not glucagon-like peptide-1, is cleared exclusively by glomerular filtration in anaesthetised pigs. *Diabetologia.* 2006; 49: 706-712.
145. Plamboeck A, Holst JJ, Carr RD and Deacon CF. Neutral endopeptidase 24.11 and dipeptidyl peptidase IV are both mediators of the degradation of glucagon-like peptide 1 in the anaesthetised pig. *Diabetologia.* 2005; 48: 1882-1890.
146. Jodal A, Pape F, Becker-Pauly C, Maas O, Schibli R and Behe M. Evaluation of (1)(1)in-labelled exendin-4 derivatives containing different meprin beta-specific cleavable linkers. *PLoS One.* 2015; 10: e0123443.
147. Schottelius M and Wester HJ. Molecular imaging targeting peptide receptors. *Methods.* 2009; 48: 161-177.
148. Laverman P, Sosabowski JK, Boerman OC and Oyen WJ. Radiolabeled peptides for oncological diagnosis. *Eur J Nucl Med Mol Imaging.* 2012; 39: S78-92.
149. Reubi JC. Old and new peptide receptor targets in cancer: future directions. *Recent Results Cancer Res.* 2013; 194: 567-576.
150. Christ E, Wild D, Ederer S, Béhé M, Nicolas G, Caplin ME, Brändle M, Clerici T, Fischli S, Stettler C, Eil PJ, Seufert J, Gloor B, Perren A, Reubi JC and Forrer F. Glucagon-like peptide-1 receptor imaging for the localisation of insulinomas: a prospective multicentre imaging study. *Lancet Diabetes Endocrinol.* 2013; 1: 115-122.
151. Pach D, Sowa-Staszczak A, Jabrocka-Hybel A, Stefanska A, Tomaszuk M, Mikolajczak R, Janota B, Trofimiuk-Muldner M, Przybylik-Mazurek E and Hubalewska-Dydejczyk A. Glucagon-Like Peptide-1 Receptor Imaging with [Lys (40) (Ahx-HYNIC- (99 m) Tc/EDDA)NH 2 ]-Exendin-4 for the Diagnosis of Recurrence or Dissemination of Medullary Thyroid Cancer: A Preliminary Report. *Int J Endocrinol.* 2013; 2013: 384508.
152. Liu Q, Duan J, Zheng Y, Luo J, Cai X and Tan H. Rare malignant insulinoma with multiple liver metastases derived from ectopic pancreas: 3-year follow-up and literature review. *Oncotargets Ther.* 2018; 11: 1813-1819.
153. Parihar AS, Vadi SK, Kumar R, Mittal BR, Singh H, Bal A, Walia R, Shukla J and Sinha SK. <sup>68</sup>Ga DOTA-Exendin PET/CT for Detection of Insulinoma in a Patient With Persistent Hyperinsulinemic Hypoglycemia. *Clin Nucl Med.* 2018; 43: e285-e286.
154. Werner C, Lupp A, Drescher R, Freesmeyer M, Mireskandari M, Stoykow C, Bauschke A and Muller UA. Morphologically 'invisible' proinsulin - secreting adenoma detected by Ga-68 Exendin-4 (GLP-1 Receptor) positron emission tomography/CT. *J Med Imaging Radiat Oncol.* 2018; 62: 370-374.
155. Cuthbertson DJ, Banks M, Khoo B, Antwi K, Christ E, Campbell F, Raraty M and Wild D. Application of Ga(68) -DOTA-exendin-4 PET/CT to localize an occult insulinoma. *Clin Endocrinol (Oxf).* 2016; 84: 789-791.
156. Luo Y, Li J, Yang A, Yang H and Li F. <sup>68</sup>Ga-Exendin-4 PET/CT in Evaluation of Endoscopic Ultrasound-Guided Ethanol Ablation of an Insulinoma. *Clin Nucl Med.* 2017; 42: 310-311.
157. Gill A, Hoogwerf BJ, Burger J, Bruce S, MacConell L, Yan P, Braun D, Giaconia J and Malone J. Effect of exenatide on heart rate and blood pressure in subjects with type 2 diabetes mellitus: a double-blind, placebo-controlled, randomized pilot study. *Cardiovasc Diabetol.* 2010; 9: 6.
158. Baggio LL, Yusta B, Mulvihill EE, Cao X, Streutker CJ, Butany J, Cappola TP, Margulies KB and Drucker DJ. GLP-1 Receptor Expression Within the Human Heart. *Endocrinology.* 2018; 159: 1570-1584.
159. Christ E, Wild D and Reubi JC. Glucagonlike peptide-1 receptor: an example of translational research in insulinomas: a review. *Endocrinol Metab Clin North Am.* 2010; 39: 791-800.
160. Velikyan I. Radionuclides for Imaging and Therapy in Oncology. In: CHEN X, WONG S, editors. *Cancer Theranostics.* 2014; 285-325.
161. Elksnis A, Martinell M, Eriksson O and Espes D. Heterogeneity of Metabolic Defects in Type 2 Diabetes and Its Relation to Reactive Oxygen Species and Alterations in Beta-Cell Mass. *Front Physiol.* 2019; 10: 10.3389.
162. Kang NY, Soetedjo AAP, Amiruddin NS, Chang YT, Eriksson O and Teo AKK. Tools for Bioimaging Pancreatic beta Cells in Diabetes. *Trends Mol Med.* 2019; 25: 708-722.
163. Eich T, Eriksson O, Lundgren T and Nordic Network for Clinical Islet T. Visualization of early engraftment in clinical islet transplantation by positron-emission tomography. *N Engl J Med.* 2007; 356: 2754-2755.
164. Fani M, Peitl PK and Velikyan I. Current Status of Radiopharmaceuticals for the Theranostics of Neuroendocrine Neoplasms. *Pharmaceuticals.* 2017; 10: 10.3390/ph10010030.